FLOW IN A PARALLEL-PLATE CHANNEL WITH ONE MOVING WALL

A thesis submitted to the Department of Mechanical Engineering for partial fullfilment of the requirements for M.Sc. Engineering (Mechanical) degree.

by

K.B.M.Quamruzzaman

Department of Mechanical Engineering, Bangladesh University of Engineering and Technology, Dacca, Bangladesh.

1973

FLOW IN A PARALLEL-PLATE CHANNEL

WITH ONE MOVING WALL

by

K.B.M.Quamruzzaman

has been approved.

November 1973

APPROVED :

Chairman

Obaidul Islam

This is certified that this work was done by me and it was not submitted anywhere else for the award of any degree or diploma or for publication.

Mushtaq Husain Khan

Signature of the Supervisor

K.B.M.Q.Z

Signature of the Candidate

ACKNWOLEDGEMENTS

With deep sense of gratitude, I acknwoledge the valuable guidance, advice, encouragement and instructions given by Dr. M.H.Khan, Professor and Head of the Department of Mechanical Engineering, B.U.E.T., who took constant interest in supervising this work.

My grateful acknwoledgements are also due to Dr, Wahhajuddin, Associate Professor, ME Deptt., Dr. Obaidul Islam, Professor, ME Deptt., Dr. Shamsul Alam, Professor, ME Deptt. and Mr. Ali Ashraf, Asstt. Professor, Mathematics Deptt. for their valuable helps and instructions obtained in course of this work.

I would also take this opportunity to thank Professor E.M.Sparrow, Deptt. of Mechanical Engineering, University of Minnesota, U.S.A. for kindly sending some of his papers in the relevant field.

Finally, I would also like to thank the Staff of the Machine Shop of this University who co-operated and helped me in constructing the experimental set-up.

SYNOPSIS

The problem of flow in a parallel-plate channel having one moving wall was investigated analytically by Sparrow and Yu by linearization technique. They also performed an experiment with "air" as the working fluid and the results found thereof showed good agreement with the analytical solutions. In this project, experiments with water and sucrose solution were carried out to further check the validity of the linearization technique. The experimental set-up was a horizontal channel one of whose walls was an endless moving belt. The ratio of the moving wall velocity to the mean fluid velocity was varied from 0 to 0.3. Measurements were made for the pressure distribution along the length of the channel. The results obtained in this experiment agreed well with the analytical solutions and as such also compared favourably with the experimental results of Sparrow. It is therefore established that the original assumptions in linearizing the inertia terms of the momentum equation are justified and the analytical solution worked out thereof for this type of flow is valid and can be applied to fluids in general.

LIST OF SYMBOLS

C_m , D_n = Series co-efficients.

h = half height of the channel.

K = incremental pressure drop due to flow development.

p = pressure.

p_o = pressure at inlet section.

u = axial velocity component.

u_o = velocity at inlet.

u_w = velocity of moving wall.

$\bar{u}$ = mean fluid velocity.

v = transverse velocity component.

X = dimensionless axial co-ordinate.

X^* = dimensionless stretched axial co-ordinate.

x = axial co-ordinate.

x^* = stretched axial co-ordinate.

y = transverse co-ordinate.

α_i = eigen values.

ϵ = stretching factor, dx/dx^*.

η = dimensionless transverse co-ordinate, y/h.

μ = viscosity.

ν = kinematic viscosity.

ρ = density.

ω = dimensionless velocity, $u/\bar{u}$.

ω_o = dimensionless velocity, $u_o/\bar{u}$.

ω_w = dimensionless velocity, $u_w/\bar{u}$

ω_{fd} = fully developed velocity distribution.

ω^* = dimensionless difference velocity component in the developing region.

N_{Re} = Reynold's number.

CHAPTER I

INTRODUCTION

This thesis work was an attempt to investigate some aspects of laminar flow development in a parallel-plate channel having one of its walls moving. This type of flow is generally known as "Couette flow" and it is the result of superposition of simple shear flow over parallel flow between two flat walls. For this type of flow with a constant pressure gradient in the axial direction, an exact solution of the Navier Stoke's equation can be found giving the transverse velocity profile. The equation for the axial velocity "u" comes out in terms of the constant pressure gradient "dp/dx", the transverse co-ordinate "y", the wall velocity "u_w" and other fluid characteristics.

The pressure gradient in a channel flow, however, does not remain constant until the velocity profile is fully developed. The velocity profile, which is rectangular at the entrance, undergoes changes in subsequent sections and after certain distance, attains a parabolic shape. The flow then becomes "fully developed", and the velocity profile remains unchanged thenceforth for the rest of the length of the channel.

The qualitative behaviour of the flow in this "hydrodynamic entrance region" of ducts and channels can be explained as follows :

Fluid enters the duct with a velocity profile that is determined by the upstream conditions. At some distance downstream from the inlet section, the fluid velocity near the walls has decreased, and to maintain continuity, the velocity in the central portion has increased. After certain section downstream, the fluid velocity no longer change with axial distance and the flow has become fully developed. The development region or the entrance region encompasses that portion of the duct length which is required for attainment of fully developed conditions. The axial pressure gradient is higher in the entrance region than at duct sections where the flow is developed because of the following effects :

a) The increase in momentum of the fluid as the velocity distribution becomes less uniform. It may be mentioned that the ratio of momentum for parabolic profile to that for rectangular profile (for equal flow rates) is 1.2 .

b) The higher wall shear caused by higher transverse velocity gradients.

Investigations have been carried out on developing flows or in other words on flow in the entrance region of ducts of circular cross-section and ducts with stationery walls. Investigation of flow beyond the entrance region i.e. in the developed region dates back to as early as the times of G.Hagen (1)* and J.Poisseuille (2) who in 1839 and 1841 respectively, separately worked out equations for volume flow-rates for laminar flow through circular pipes. Literature on flow-development

* Numerals in parentheses refer to bibliography.

in the entrance region of tubes and ducts are presented later in this thesis.

In this thesis, however, flow conditions both in the entrance as well as in the developed regions in a parallel-plate channel having one of its walls moving parallel to the flow direction were studied. An analytical solution of this particular problem was worked out by Professor E.M.Sparrow and H.S.Yu (3) employing a linearized model of the momentum equation.

In the present work, the aforesaid analytical solution for axial pressure distribution has been verified in an experimental set-up with such dimensions and design so as to facilitate the use of different liquids as the working substance.

The objective of this thesis work was experimental investigation of the analytical solution given by Sparrow and Yu for flow in a parallel-plate channel having one moving wall. The working substances used were water and sucrose solution. Thus results of experiments with three different fluids, with water and sucrose solution obtained from this project and with air found by Sparrow and Yu were at hand to study the effect of such fluid properties as viscosity and density on the results.

The experiments covered the range of $u_w/\bar{u}$ from 0 to .3 and the Reynold's number range (based on channel gap) from about 780 to 2030. Static pressure measurements were compared with the pressure-drop predictions obtained from the analysis. As will be shown later, very good agreement was found between them, thereby lending support to the analytical solution.

CHAPTER II

REVIEW OF LITERATURE

The study of fluid flow in ducts in the developed region dates back to as early as 1839. G.Hagen (1) in 1839 and J.Poisseuille in 1841, independently worked out equations for the volume flow-rates for laminar flow through circular pipes. The equation, known as Hagen-Poisseuille equation of laminar flow through a pipe, expresses the volume flow-rate Q in terms of the pipe diameter, the pressure gradient "dp/dx" and the fluid viscosity "μ". Both Hagen and Poisseuille arrived at the equation by making the force balance in the axial direction on a co-axial fluid cylinder in a circular pipe. The equation can also be obtained from the Navier Stoke's equation.

Flow in the inlet lengths of ducts was studied extensively and different approaches were made. To provide perspective to the present investigation, a brief discussion of the different approaches to the entrance region problem is given.

One method of analysis was to apply the integral representation of the equation of motion and of continuity to the boundary layers which developed along the duct walls. The velocity profile was written in a polynomial form as in the standard Karman-Pohlhausen method. The initial application of this approach to tubes and channels was due to Shiller(4) with later modifications and improvements due to Campbell and Slattery(5).

The second approach subdivided the entrance region into two zones. In the zone near the tube entrance, a boundary layer model was proposed. In the next zone beyond the entrance region, solutions were obtained as perturbations of the fully developed velocity distribution. This later solution was first proposed by Boussinesq (6). Schlicting (7) in 1934 combined these two solutions to get flow development throughout the entrance region. First, he made the integration from the inlet section in the downstream direction so that the boundary layer growth was calculated for an accelerated external stream. Then the integration was done in the reverse direction from a section in the fully developed zone, analysing the progressive deviation of the velocity profile from its asymptotic distribution of Poisseüille flow. Having obtained both solutions, in the form of series expansions, sufficient number of terms in both the series were retained and combined for a section where both the series were still applicable. In this way expression for flow for the whole inlet length was obtained.

The same "patching up" method of the two solutions were later applied by Atkinson and Goldstein(8) for the circular tube.

A third and altogether different approach of the problem of flow development was achieved by linearizing the inertia terms of the equations governing the flow development. With this, a boundary-layer model need not be postulated. Rather, velocity expressions which are continuous over the cross-section and along the length all the way from the duct entrance to the fully developed region, were obtained.

In a paper, "Flow development in the hydrodynamic entrance region of tubes and ducts" by Sparrow, Lin and Lundgren(9), an analysis of the developing flow in ducts of arbitrary cross-section was made using the linearization technique.

The solution for the velocity field was first found out. With the solution for the velocity field at hand, expression for pressure drop was then found by integrating the momentum equation. Then from the generalized equations, results for two ducts namely circular tube and parallel-plate channel, were derived.

Experimental verification of the above analytical model was carried out by Sparrow, Hixon and Shavit and was reported in reference (10). The experiments were performed for rectangular ducts of two aspect ratios, 5:1 and 2:1 with air as the working fluid. Velocity profiles at a large number of stations in the entrance region were measured across the duct cross-section. In addition, measurements for the axial pressure distribution were also made. The lengths of the hydrodynamic entrance region were theninferred from the velocity and pressure data.

In another subsequent paper by Sparrow and Flemming (11), a general method of analysis was presented for determining the developing velocity field and pressure drop for laminar flow in the entrance region of ducts having arbitrary cross-sections. In addition, the general solution was applied to rectangular and triangular ducts and velocity field and pressure drop results were presented and compared with available informations. Finally analytical results for the development of the velocity and pressure fields for several ducts were compiled together and general trends were indicated.

In the paper "Flow development in a parallel-plate channel having a longitudinally moving wall" by Sparrow and Yu (3), the above mentioned linearization method was extended to generalize the analytical solution for the developing velocity field in the presence of a moving wall. An experiment was performed in a channel, one of whose walls was the surface of a rotating cylinder functioning as the moving wall. Air was the workingfluid. Measurements were made for the pressure distribution along the length of the channel. The experimental results found thereof lent good support to the analytical model.

In this work, the analytical solution given by Sparrow and Yu was used. The salient features of the analytical solution are given in Chapter III.

CHAPTER III

THEORY

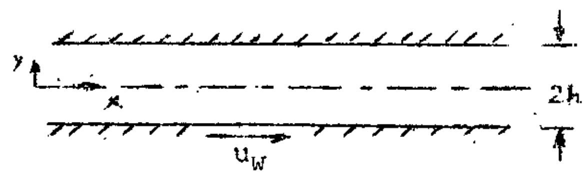

Fig. 1 Schematic of a parallel-plate channel having a moving wall.

Let us consider flow through the parallel-plate channel shown in fig. 1. Distances "x" are measured along the axis of the channel from a section x = 0, where the velocity profile is known. Transverse distances "y" are measured from the axis of the channel, the total width of the channel being "2h". Lower wall moves with a velocity u_W.

The case being that of a steady, incompressible, 2-dimensional motion, the differential equations governing the flow are :

$$u \frac{\partial u}{\partial x} + v \frac{\partial u}{\partial y} = -\frac{1}{\rho} \frac{dp}{dx} + \nu \frac{\partial^2 u}{\partial y^2} \qquad \text{.......(1)}$$

and

$$\frac{\partial u}{\partial x} + \frac{\partial v}{\partial y} = 0 \qquad \text{.......(2)}$$

Professor Sparrow and co-worker used a linearized model to solve for the flow development in this particular case. Thus equation (1) in the linearized form was rewritten as :

$$\epsilon(x)\, \bar{u} \frac{\partial u}{\partial x} = \Lambda(x) + \nu \frac{\partial^2 u}{\partial y^2} \qquad \text{.......(3)}$$

Where $\epsilon(x)$ is a function weighting the mean velocity " $\bar{u}$ " to compensate for the velocity component "u" . $\Lambda(x)$ is another function accounting for the pressure gradieant and the residual of the inertia terms.

Now combining (2) and (3) we have :

$$-\epsilon(x)\,\bar{u}\,\frac{\partial v}{\partial y} = \Lambda(x) + \nu\frac{\partial^2 u}{\partial y^2} \qquad \text{.........(4)}$$

Integration of (4) within the limits $-h \leq y \leq h$ gives :

$$-\epsilon(x)\,\bar{u}\,.\,v\Big]_{y=-h}^{y=+h} = \Lambda(x)\,y\Big]_{-h}^{+h} + \nu\frac{\partial u}{\partial y}\Big]_{-h}^{+h}$$

$$\text{or,}\quad \Lambda(x) = -\frac{\nu}{2h}\left[\left(\frac{\partial u}{\partial y}\right)_h - \left(\frac{\partial u}{\partial y}\right)_{-h}\right] \qquad \text{........(5)}$$

[v is zero on the walls]

A stretched axial co-ordinate x^* is now introduced with the definition:

$$dx = \epsilon(x)\,dx^* \qquad \text{........(6)}$$

Also the following dimensionless variables are introduced :

$$\omega = \frac{u}{\bar{u}} \;;\; \eta = \frac{y}{h} \;;\; X = \frac{x\nu}{\bar{u}\,h^2} \quad \text{and} \quad X^* = \frac{x^*\nu}{\bar{u}\,h^2}$$

Equations (4) and (5) gives :

$$\epsilon(x)\,\bar{u}\,\frac{\partial u}{\partial x} = -\frac{\nu}{2h}\left[\left(\frac{\partial u}{\partial y}\right)_h - \left(\frac{\partial u}{\partial y}\right)_{-h}\right] + \nu\frac{\partial^2 u}{\partial y^2} \qquad \text{.......(7)}$$

Using the dimensionless variables as stated above, Equation (7) reduces to (shown in Appendix III(1)) :

$$\frac{\partial \omega}{\partial X^*} + \frac{1}{2}\left[\left(\frac{\partial \omega}{\partial \eta}\right)_{+1} - \left(\frac{\partial \omega}{\partial \eta}\right)_{-1}\right] = \frac{\partial^2 \omega}{\partial \eta^2} \qquad \text{......(8)}$$

Equation (8) is a linear equation governing the flow development in terms of the dimensionless variables explained earlier. It provides a means for determining the velocity distribution as a function of the stretched axial co-ordinate X^* and the transverse co-ordinate η .

Let us seek the solution of equation (8) in the form of :

$$\omega(X^*, \eta) = \omega_{fd}(\eta) + \omega^*(X^*, \eta) \quad \text{.........(9)}$$

where ω_{fd} is the fully developed velocity distribution, independent of the axial co-ordinate and a function of the transverse co-ordinate only. ω^* is a difference velocity which embodies the developmental component of the velocity field.

Now, eqn. (8) with the term $\frac{\partial \omega}{\partial X^*}$ deleted is an exact representation of momentum equation for fully developed flow. Hence the solution of the eqn.,

$$\frac{\partial^2 \omega}{\partial \eta^2} = \frac{1}{2}\left[\left(\frac{\partial \omega}{\partial \eta}\right)_1 - \left(\frac{\partial \omega}{\partial \eta}\right)_{-1}\right] \quad \text{.......(10)}$$

yields ω_{fd} .

Integrating eqn. (10) and using the boundary condition $\omega = 0$ at $\eta = +1$ one gets (App. III(2)) :

$$\omega = \frac{1}{4}\left[\left(\frac{\partial \omega}{\partial \eta}\right)_1 - \left(\frac{\partial \omega}{\partial \eta}\right)_{-1}\right]\eta^2 + \frac{1}{2}\left[\left(\frac{\partial \omega}{\partial \eta}\right)_1 + \left(\frac{\partial \omega}{\partial \eta}\right)_{-1}\right]\eta - \left[\frac{3}{4}\left(\frac{\partial \omega}{\partial \eta}\right)_1 + \frac{1}{4}\left(\frac{\partial \omega}{\partial \eta}\right)_{-1}\right] \quad \text{—(11)}$$

Condition $\omega = \omega_w$ at $\eta = -1$ gives :

$$\omega_w = -\left[\left(\frac{\partial \omega}{\partial \eta}\right)_1 + \left(\frac{\partial \omega}{\partial \eta}\right)_{-1}\right] \quad \text{—(12)}$$

Again writing expression for $\bar{u}$ we have the relation :

$$\bar{u} = \frac{1}{2h}\int_{-h}^{+h} u\,dy$$

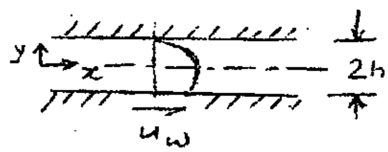

fig.2 velocity profile in Couette flow.

or, $$\frac{1}{2}\int_{-1}^{+1} \omega \, d\eta = 1 \quad \text{—— (13)}$$

Eqns. (11) + (13) gives (App. III (3)) :

$$2\left(\frac{\partial \omega}{\partial \eta}\right)_1 + \left(\frac{\partial \omega}{\partial \eta}\right)_{-1} = -3 \quad \text{—— (14)}$$

combining (12) + (14) one gets :

$$\left(\frac{\partial \omega}{\partial \eta}\right)_1 = \omega_w - 3 \quad \text{—— 15(a)} \quad +$$

$$\left(\frac{\partial \omega}{\partial \eta}\right)_{-1} = -2\omega_w + 3 \quad \text{—— 15(b)}$$

Eqns. (15(a)), (15(b)) with eqn.(11) gives solution for ω_{fd} as

$$\omega_{fd} = \frac{3}{4}(\omega_w - 2)\eta^2 + \frac{1}{2}\omega_w \eta + \frac{3}{2} - \frac{1}{4}\omega_w \quad \text{—— (16)}$$

The difference velocity fn. ω^* obeys eqn. (8). A seperable solution for it is sought in the form :

$$\omega^*(x^*, \eta) = f(x^*)\, g(\eta) \quad \text{—— (17)}$$

substituting in eqn. (8) one gets :

$$f' + \lambda^2 f = 0 \quad \text{—— (18)} \quad \text{and}$$

$$g'' + \lambda^2 g = \frac{1}{2}[g'(1) - g'(-1)] \quad \text{—— (19)}$$

Eqn. (18) has the solution :

$$f = C_1 e^{-\lambda^2 x^*} \quad \text{—— (20)}$$

Now, at $\eta = \pm 1$ we have $\omega^* = 0$

Therefore, $g(-1) = g(1) = 0$

This implies that g equation (eqn. 19) and its boundary conditions constitute an eigen-value problem.

General solution of eqn. 19 is (App. III(4)) :

$$g = A\cos\lambda\eta + B\sin\lambda\eta + \frac{1}{2\lambda^2}\left[g'(1) - g'(-1)\right] \quad \ldots\ldots(21)$$

Differentiating eqn. 21 and arranging one gets :

$$g'(1) - g'(-1) = -2A\lambda\sin\lambda$$

Eqn. 21 can now be reduced to :

$$g = B\sin\lambda\eta + A\left[\cos\lambda\eta - \frac{\sin\lambda}{\lambda}\right] \quad \ldots\ldots(22)$$

Boundary conditions $g(1) = g(-1) = 0$ gives :

$$2B\sin\lambda = 0, \quad \therefore \lambda = n\pi, \quad n = 1, 2, 3 \ldots\ldots$$

$$\text{and} \quad 2A\left[\cos\lambda - \frac{\sin\lambda}{\lambda}\right] = 0 \quad \text{whence,} \quad —(23)$$

$$\tan\lambda = \lambda \quad \text{implying that} \quad \lambda \to 0 \quad —(24)$$

Using eqn. 24 we can write eqn. 22 as :

$$g = B\sin\lambda\eta + A\left[\cos\lambda\eta - \cos\lambda\right] \quad —(25)$$

The flow model does not possess centre-line symmetry. Therefore consideration must be given to both the symmetric and the anti-symmetric eigen-functions. From eqn. 25 it is obvious that the anti-symmetric eigen-functions and eigen-values are :

$$G_n = \sin n\pi\eta, \quad \lambda_n = n\pi \quad (n = 1, 2, 3 \ldots) \ldots\ldots(26)$$

The symmetric eigen-functions and the corresponding eigen-values include the cosine terms. After rearraging (App. III(5)) and multiplying by $\frac{1}{\alpha_m}$ in order to normalize, this can be written as :

$$g_m = \frac{1}{\alpha_m}\left[1 - \frac{\cos \alpha_m \eta}{\cos \alpha_m}\right], \qquad \begin{matrix} \lambda_m = \alpha_m \text{ and} \\ \lambda_m = \tan \lambda_m \end{matrix}$$

$$[m = 1, 2, 3 \ldots\ldots] \quad \text{—(27)}$$

Both sets of eigen-functions are normalized so that (App. III(6)(a) and (b)),

$$\int_{-1}^{+1} g_m^2 \, d\eta = \int_{-1}^{+1} G_n^2 \, d\eta = 1 \qquad \ldots\ldots(28(a)).$$

Also it may be readily verified that the eigen-functions possess the following orthogonality properties (App. III(7)(a)).

$$\int_{-1}^{+1} g_m G_n \, d\eta = 0 \qquad \text{for all values of m \& n} \quad \ldots\ldots(28(b)).$$

and (App. III(7)(b) & (c)),

$$\int_{-1}^{1} g_m g_i \, d\eta = \int_{-1}^{1} G_n G_j \, d\eta = 0 \qquad m \neq i,\ n \neq j \quad \ldots\ldots(28(c)).$$

The general solution for ω^* combining the results of (20), (26) and (27) is,

$$\omega^*(x^*, \eta) = \sum_{m=1}^{\infty} C_m g_m(\eta)\, e^{-\alpha_m^2 X^*} + \sum_{n=1}^{\infty} D_n G_n(\eta)\, e^{-n^2\pi^2 X^*} \qquad \ldots\ldots(29)$$

Let us now assume that the velocity profile at x = 0 is known and is,

$u = u_o(y)$ or $\omega = \omega_o(\eta)$ at $X^* = 0$.

With this information, the co-efficients C_m and D_n can now be evaluated as follows :

Using eqns (9), (16) and (29) we have,

$$\omega_o(\eta) = \omega_{fd}(\eta) + \sum_{m=1}^{\infty} C_m g_m(\eta) + \sum_{n=1}^{\infty} D_n G_n(\eta) \quad ...(30)$$

Multiplying eqn. (30) by $g_i(\eta)$ and integrating over the range $-1 \leq \eta \leq 1$ and upon utilising the orthogonality properties (28(a)), (28(b)) and (28(c)) and the expression for ω_{fd} from eqn. (16) we find that (App.III(8)(a)),

$$C_m = \int_{-1}^{+1} \frac{\omega_o(\eta)}{\alpha_m} d\eta - \frac{2}{\alpha_m} + \frac{1}{\alpha_m}\left[\omega_\omega - \int_{-1}^{+1} \omega_o(\eta) \frac{\cos \alpha_m \eta}{\cos \alpha_m} d\eta\right] \quad ....(31(a))$$

Similarly D_n is found by multiplying eqn.(30) by $G_j(\eta)$ and integrating (App. III(8)(b)),

$$D_n = -\frac{(-1)^n}{n\pi} \omega_w + \int_{-1}^{+1} \omega_o(\eta) \sin n\pi\eta \, d\eta \quad .....(31(b))$$

The complete solution for the velocity field may now be written as :

$$\omega = \frac{3}{4}(\omega_\omega - 2)\eta^2 - \frac{1}{2}\omega_\omega \eta + \frac{3}{2} - \frac{1}{4}\omega_\omega + \sum_{m=1}^{\infty} \frac{C_m}{\alpha_m}\left[1 - \frac{\cos \alpha_m \eta}{\cos \alpha_m}\right] \times e^{-\alpha_m^2 X^*} + \sum_{n=1}^{\infty} D_n \sin n\pi\eta \, e^{-n^2\pi^2 X^*} \quad ....(32)$$

Where the co-efficients C_m and D_n are given by eqns. (31(a)) and (31(b)).

Expression for pressure distribution :

To find the pressure distribution along the length of the duct, we use the momentum eqn. First the inertia terms in eqn.(1) are re-phrased as :

$$\frac{\partial}{\partial x}(u^2) + \frac{\partial}{\partial y}(u v)$$

Then the thus modified eqn.(1) is integrated across the section, giving (App. III (9)),

$$-\frac{1}{\rho \bar{u}^2}\frac{dp}{dx} = \frac{1}{2}\frac{d}{dx}\int_{-1}^{1} \omega^2 d\eta - \frac{1}{2}\left[\left(\frac{\partial \omega}{\partial \eta}\right)_1 - \left(\frac{\partial \omega}{\partial \eta}\right)_{-1}\right] \qquad (33)$$

or, $$-\frac{1}{\epsilon \rho \bar{u}^2}\frac{dp}{dx^*} = \frac{1}{2\epsilon}\frac{d}{dx^*}\int_{-1}^{1} \omega^2 d\eta - \frac{1}{2}\left[\left(\frac{\partial \omega}{\partial \eta}\right)_1 - \left(\frac{\partial \omega}{\partial \eta}\right)_{-1}\right] \qquad (34)$$

Integration of this eqn. between the sections $x=0$ and $x=x$ [i.e. $p=p_0$ at $x^*=0$ & $p=p$ at $x^*=x^*$] gives (App. III (10)),

$$\frac{p_0-p}{\frac{1}{2}\rho\bar{u}^2} = 3(2-\omega_\omega)x + \int_{-1}^{1}\omega^2 d\eta - \int_{-1}^{1}\omega_0^2 d\eta$$
$$- \int_0^{x^*}\left[\left(\frac{\partial \omega^*}{\partial \eta}\right)_1 - \left(\frac{\partial \omega^*}{\partial \eta}\right)_{-1}\right]\epsilon\, dx^*$$

or, we can write:

$$\frac{p_0-p}{\frac{1}{2}\rho\bar{u}^2} = \frac{(p_0-p)_{fd}}{\frac{1}{2}\rho\bar{u}^2} + K(x) \qquad (35)$$

where $\frac{(p_0-p)_{fd}}{\frac{1}{2}\rho\bar{u}^2} = 3(2-\omega_\omega)\frac{x\nu}{\bar{u}h^2}$ and

$$K(x) = \int_{-1}^{1}\omega^2 d\eta - \int_{-1}^{1}\omega_0^2 d\eta - \int_0^{x^*}\left[\left(\frac{\partial \omega^*}{\partial \eta}\right)_1 - \left(\frac{\partial \omega^*}{\partial \eta}\right)_{-1}\right]\epsilon\, dx^*$$

Equation (35) gives an expression for pressure difference between the entrance section and any downstream section. The term $(p_0-p)_{fd}/\frac{1}{2}\rho\bar{u}^2$ represents the pressure drop that would be sustained by the flow if it were fully developed right from the duct inlet. The quantity $K(x)$ represents the incremental pressure drop due to flow development.

To facilitate the evaluation of the pressure from eqn. (35), the factor $K(x)$ is expressed in terms of the velocity solution as given in eqn. (32). Thus after substitution and indicated operation,

$$K(x) = \frac{4}{15}\,\omega_w^2 - \frac{2}{5}\,\omega_w + \frac{12}{5} + 2\,(2-\omega_w)\sum_{m=1}^{\infty}(C_m/\alpha_m)\,e^{-\alpha_m^2 X^*}$$

$$+\,2\,\omega_w \sum_{n=1}^{\infty} \frac{(-1)^n}{n\pi}\, D_n\, e^{-n^2\pi^2 X^*} + \sum_{m=1}^{\infty} C_m^2\, e^{-2\alpha_m^2 X^*}$$

$$+\sum_{n=1}^{\infty} D_n^2\, e^{-2n^2\pi^2 X^*} - \int_{-1}^{1} \omega_0^2\, d\eta - 2\int_0^{X^*}\left[\sum_{m=1}^{\infty} C_m \alpha_m e^{-\alpha_m^2 X^*}\right] \times \epsilon\, dX^* \qquad \text{—(36)}$$

In their paper, Prof. Sparrow and H.S.Yu evaluated $K(x)$ assuming $\omega_0(\eta) = 1$ for a wide range of operating conditions and have presented the results in graphical form. For the calculations of the incremental pressure drop $K(x)$ in the development region in our case, we will use this graph.

The pressure gradient in the fully developed region can also be deduced from the basic equations for Couette flow.

The pressure gradient remaining constant, the equation of motion in this case can be written as :

$$\mu \frac{d^2 u}{d y^2} = \frac{dp}{dx} = \text{Constant} \qquad \ldots\ldots(37)$$

Integration of this equation with the boundary conditions,

$y = h$, $u = 0$ and $y = -h$, $u = u_w$ yields,

$$\mu(u) = \frac{dp}{dx}\,\frac{y^2}{2} - \frac{\mu u_w}{2h}\,y + \frac{1}{2}\left[\mu u_w - \frac{dp}{dx}h^2\right]$$

Writing the expression for $\bar{u}$.

$$\bar{u} = \frac{1}{2h}\int_{-h}^{+h} u\,dy$$

and putting the expression for u from eqn. (38) one obtains,

$$\frac{dp}{dx} = \frac{3\mu}{2h^2}\left(u_w - 2\bar{u}\right)$$

It is interesting to note that eqn.(39) when converted into an equation of dimensionless quantities becomes,

$$\frac{(P_o - P)_{fd}}{\frac{1}{2}\rho\bar{u}^2} = 3\left(2 - \omega_w\right)\frac{x\nu}{\bar{u}h^2}$$

which is the same equation for dimensionless pressure and axial distance for fully developed flow as derived earlier in eqn. (35) by linearization technique.

CHAPTER IV

THE EXPERIMENTS

The experimental set-up : A general view of the experimental set-up is given in Plate No. 1. The set-up consisted mainly of a parallel-plate channel, a means of driving a belt which served as the moving wall and a bank of vertical glass tubes for measuring the static pressures. A schematic diagram of the test section is shown in Fig. 2.

The test section consisted of a horizontal parallel-plate channel made of two teak wood plates with 0.122 inch gap and 4.01 inches width. Along the lower wall of the channel moved an endless polythene-sheet belt, functioning as the moving wall. The upper plate had the dimensions of $22\frac{1}{2}'' \times 5'' \times \frac{3}{4}''$, those of the lower plate being $20\frac{1}{4}'' \times 5'' \times \frac{3}{4}''$. The surfaces of the wooden plates were first finished in a milling machine and were then wax-polished so that the working liquids may not soak them.

Along the centre line of the upper plate, there were drilled, 12 pressure tappings. The first tap was at a distance of 1 inch from the liquid inlet tap, the rest being spaced $1\frac{1}{2}$ inches apart with a margin of 3 inches from the last tap to the exit of the channel.

Each pressure tap, as shown in Fig. 3, consisted of two 3/64 inch

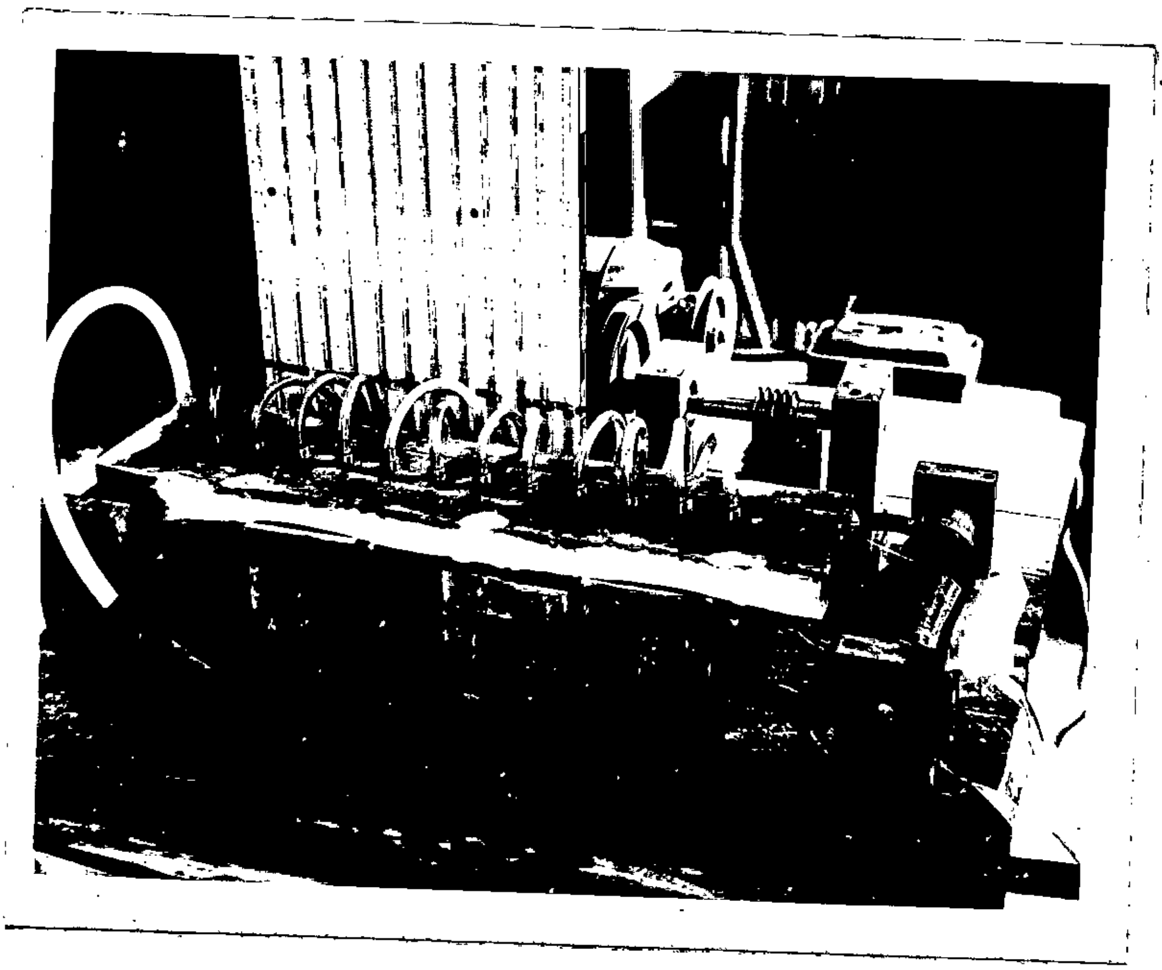

Plate No. 1 General view of the Experimental facilities.

Plate No. 2 Split view of the Channel.

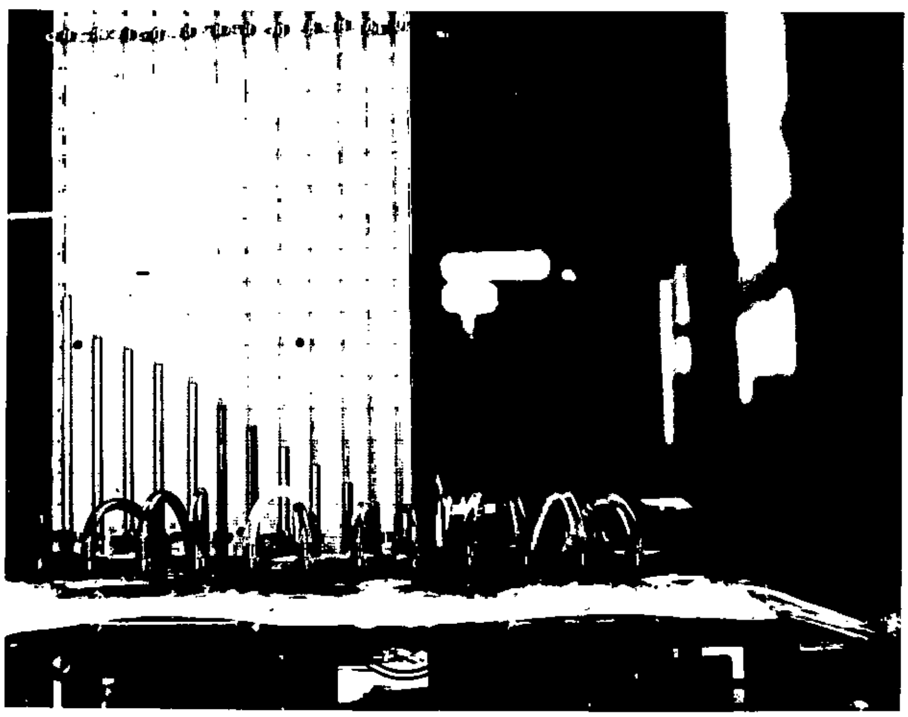

Plate No. 3 Manometer bank during experiments.

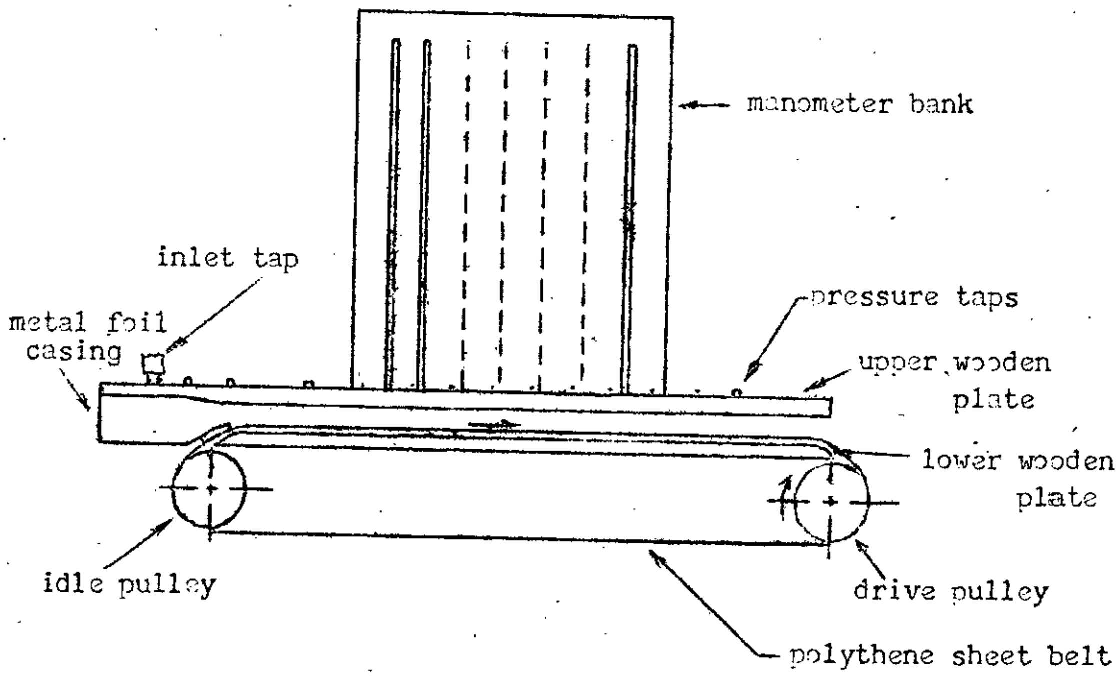

Fig. 2 Schematic diagram of the test-section

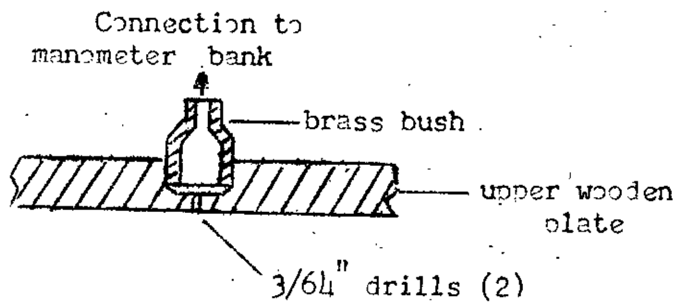

Fig. 3 Sectional view of a pressure tap

drills, connected to a brass bush which in turn was connected with the manometer bank. Two drills for each pressure tap, placed at same axial distance, were used to average out any fluctuation in the pressure readings.

The 3/64 inch dia. drills were found to be optimum for the press. taps. These were chosen after experimenting in a channel with similar gap. The smaller size lacked quick response to change in pressures while the larger size drills showed fluctuations in readings.

The liquid inlet was through a 3/8 inch dia. tap, the centre of which was at a distance of 7/8 inch from the leading edge of the channel. The liquid first entered a casing, formed by a 1 mm thick foil, which was screwed to the upper plate on three sides. This casing gradually converged upto the leading edge of the channel, where an extension of the foil with a thin layer of sponge attached to its lower side, pressed on the moving polythene belt. This arrangement allowed the belt to move freely but made the entrance side of the channel leak-proof.

As mentioned earlier, the function of the moving wall was performed by an endless polythene-sheet belt, 3.9 inches in width. The belt was made by glueing the two ends of a polythene sheet, 3.9 inches wide and of requisite length, the lap being 1.3 inches. The two ends were made thinner so that after they were lapped, the thickness did not vary appreciably from that of the single sheet.

The belt was driven by a motor (1/3 hp; 1425 rpm). The speed was reduced 4 times in the first step by pulleys and a V-belt. Then 24 times reduction was obtained through a worm gear drive. Step pulleys were used for the final drive. In the step pulleys, three steps were provided to give belt speeds of .1834 fps, .225 fps and .283 fps. While being driven the belt glided along the surface of the lower plate.

Parallel grooves were cut cross-wise on the surface of the lower plate (as shown in Plate No. 2) to avoid film shear. With the surface of the lower plate being plane, the moving belt sheared the film of the working liquid in between the lower plate and the belt. The film thickness being very small , and the surface area of the lower plate being large, the shear force arising out of this film shear became considerable. With the working speed of the belt , this shear force held back the belt and caused it to slip over the pulleys. The grooves, cut along the entire length of the lower plate, in effect, cut this film of the working liquid and thereby the adverse shear force was eliminated, allowing the belt to move over the lower plate smoothly without slip.

The whole set-up was installed on a 30" x 20" wooden board having rubber paddings to damp out any vibrational effect arising from the rotating parts.

The experimental procedure :

In all, 13 sets of readings were taken, 9 with water and 4 with sucrose solution. With water, three sets of data were taken for zero wall speed while for each wall speeds of .1834 fps, .225 fps and .283 fps, two sets of data were recorded. The three observations for zero wall speed were with arbitrary flow-rates. But while taking readings with the wall in motion, the flow -rates , which were pre-calculated so that the parameter $u_w/\bar{u}$ had the round values of .1, .2, .3, were attained by trial. Once the flow-rate was so adjusted that $u_w/\bar{u}$ reached its value within a tolerance of ± .002, readings for pressure distribution were taken from the manometer bank.

Flow-rates were measured by collecting the liquid at the exit of the channel. Care was taken to arrest any liquid escaping the collecting tray either by dropping through the sides or flowing to the rear by adhering to the moving belt.

The lap-joint of the moving belt, while inside the channel, disturbed the flow and consequently the pressure readings were also disturbed. Data for pressures were therefore read while the readings in the manometer bank were steady during the interval the joint came out of the exit and again entered the channel.

Before taking readings, the manometer tubes were flushed to ensure that there was no air-bubble inside them.

While experimenting with water, tap water from overhead tank was directly introduced in the entrance section casing. But with sucrose solution, the whole set-up was placed in conjunction with a hydraulic bench and the same liquid was recirculated by a pump.

Operating temperatures during experiments with water was 81°F which corresponded the ambient temperature at that time. While experimenting with sucrose solution, the temperature of the liquid was kept at 65°F so that the viscosity was more and differed considerably from that of water at 81°F.

CHAPTER V

RESULTS AND DISCUSSION

The experimental data sheet, the analytical results in tabular form and a sample calculation for Observation No. 2-2 have been shown in the Appendix in sections (V-2),(V-3) and (V-3) respectively.

Discussion on exit error correction :

In finding the pressures at different sections, the experimental pressure at tap No. 2 was taken as "p_o" or in other words, axial distance was measured from the section where tap No. 2 was. This section corresponded to the leading edge of the channel, that is, the channel converged at this section to its normal width, 2h = 0.122 inch.

As indicated in Chapter III, x = 0 should be reckoned from a section where the relation $u_o/\bar{u} = 1$ holds. In the set-up of this project, liquid was forced through a passage of larger gap which gradually converged at the leading edge to the normal gap of the channel. This geometry ensured the flow to attain a nearly rectangular velocity profile at the leading edge. Hence for the calculations, at first it was assumed that $u_o/\bar{u} = 1$ holds at the leading edge. However, depending on the channel geometry and flow conditions, the inlet section (x = 0) may not exactly coincide with the leading edge. To eliminate any error due to this discrepency, the informations p_{ex} (pressure at the exit) = 0 , were utilised. Thus for each set of reading, p_{ex} was calculated. The amount was then subtracted or added according as it was positive or negative, from all the calculated pressure readings. Analytical pressure for each set of data was thus found.

Discussion on results :

The experimental results of this project and also experimental data taken from Sparrow's experiments with air have been arranged and shown in graphical forms in figures 4 to 15.

Figures 4 to 7 show the distribution of pressure along the channel axis for different values of ω_ω and N_{Re} for water. Fig. 8 is a similar plot for sucrose solution. The solid lines represent the analytical pressure distribution. It is seen that as N_{Re} increases, the pressure gradient with respect to x increases for a fixed value of ω_ω.

It is evident from these graphs, that the agreement between the analytical results and the experimental values is very good and the deviations are mostly within the limits of accuracy of the experimental facilities.

The accuracy of the experimental results was limited mainly by the minimum interval upto which the pressure could be read in the manometer tubes. The minimum graduation in the manometer was 0.1 inch and readings upto 0.05 inch were taken by eye estimation. Thus approximately ± .025 inch (of the working liquid) was the limit of accuracy of the set-up for pressure readings. This meant, for a small pressure reading of .2 inch, as much as 12.5% error was possible.

In spite of this, a manometer bank showing the piezometric heads at different tap sections was used for the following considerations :

i) The readings for the pressures for a particular set of data were to be taken within a short interval of time to avoid other possible errors such as fluctuation of the head of the inlet liquid.

ii) The pressure profile could be directly seen in the manometer bank.

In Fig.9 analytical pressure distribution along the dhannel axis for same $\bar{u}$ and u_W are plotted for water and sucrose solution to see the effect of viscosity on the pressure distribution. Sucrose solution with higher viscosity has a steeper pressure gradient than that of water ($\omega_\omega = .2$; $u_W = .225$fps). This is expected from Eqn.39 in Chapter III, since all other terms remaining constant, dp/dx must increase with increase of μ .

Fig.10 is the plot of the analytical pressure vs. axial distance at same N_{Re} and different ω_ω's. It is seen that at same N_{Re}, the pressure gradient may be different depending on the value of ω_ω. Pressure gradient at zero wall speed is steeper than that when the wall is in motion at same Reynold's number.

Fig.11 is the plot of experimental values of $\frac{p_0-p}{\frac{1}{2}\rho\bar{u}^2}$ vs $\frac{x\nu}{\bar{u}h^2}$ at $\omega_w=0$ for different N_{Re} . Data for water and sucrose solution from this work and that for air from the experiments of Sparrow (3) are used in this plot.

The experimental plots clearly shows good agreement with the analytical values. It is also clear from this experiment that this plot in dimensionless co-ordinates holds for any fluid as the working substance.

Figs. 12 to 14 are plots of $\frac{p_o - p}{\frac{1}{2}\rho \bar{u}^2}$ vs. $\frac{x\nu}{\bar{u}h^2}$ at different values of ω_ω with data taken from this experiment with water and sucrose solution. The agreement of the experimental values with analysis at other values of ω_ω (.1, .2 and .3)is demonstrated in these graphs.

Fig.15 compares the present experimental results with those of Sparrow. The comparison is quite favourable although all values of ω_ω could not be covered in the present work. $\frac{p_o - p}{\frac{1}{2}\rho \bar{u}^2}$ (through a range of 0-.4) can be read from this plot for different values of $\frac{x\nu}{\bar{u}h^2}$(through a range of 0-.6) at different ω_ω's. It is seen that as ω_ω increases, the dimensionless pressure gradient with respect to dimensionless axial distance decreases.

For ω_ω=0 , data are taken from the experiments with water, sucrose solution and air. Curves for ω_ω= .1, .2 and .3 are plotted from results of the experiments performed with water and sucrose solution. Curves for ω_ω= .5,1.0 and 1.5 are drawn by taking the experimental data for air (3).

This plot in dimensionless quantities holds for any fluid. It can be used for getting information for any fluid flowing through a channel, similar to the one used in this work but may be of different dimensions.

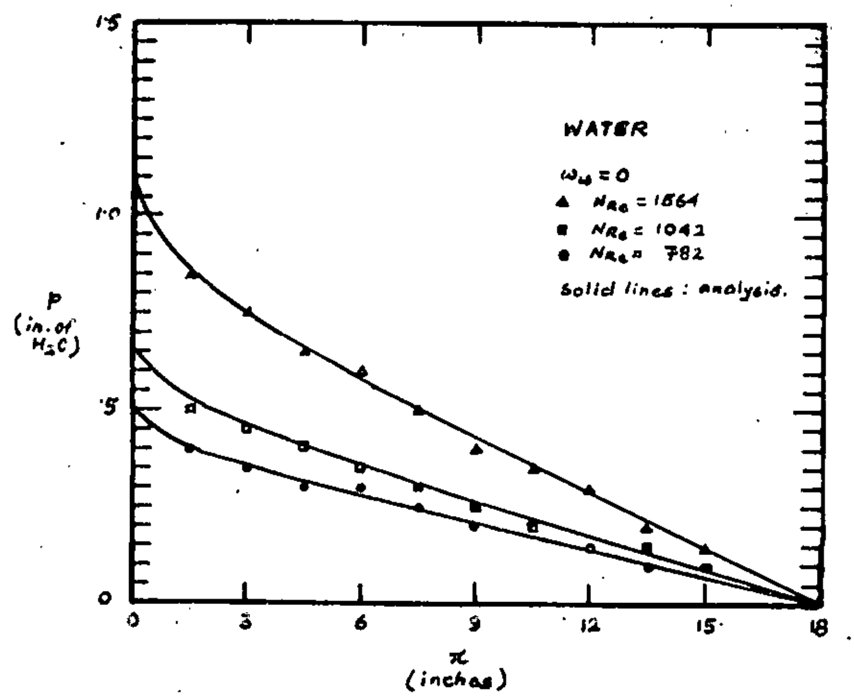
WATER
$\omega_w = 0$
$N_{Re} = 1564$
$N_{Re} = 1042$
$N_{Re} = 782$
solid lines : analysis.
p
(in. of H_2O)
x
(inches)

Fig. 4

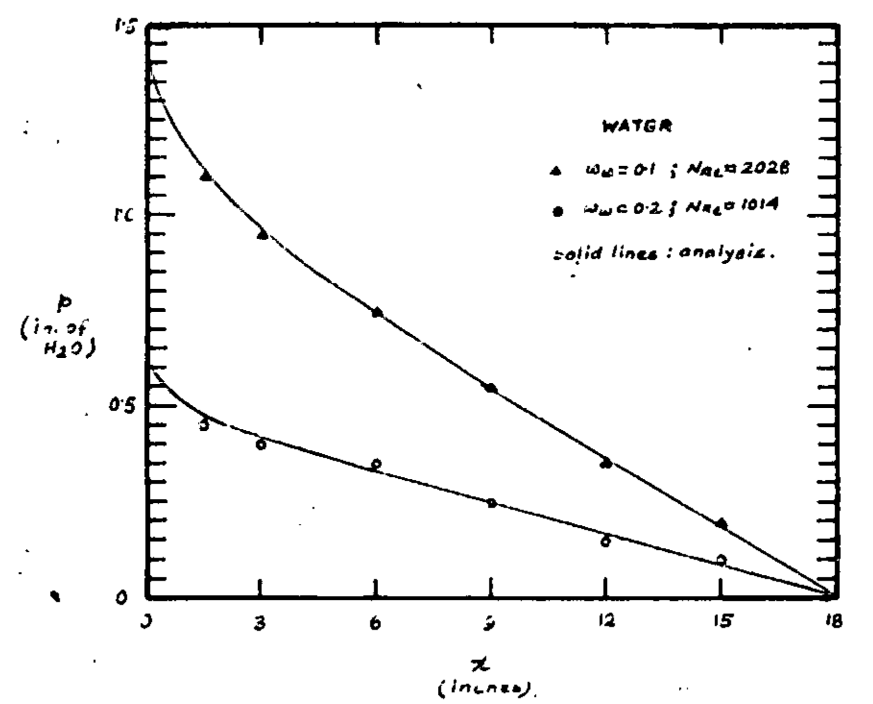
WATER
$\omega_w = 0.1$; $N_{Re} = 2028$
$\omega_w = 0.2$; $N_{Re} = 1014$
solid lines : analysis.
p
(in. of H_2O)
x
(inches)

Fig. 5

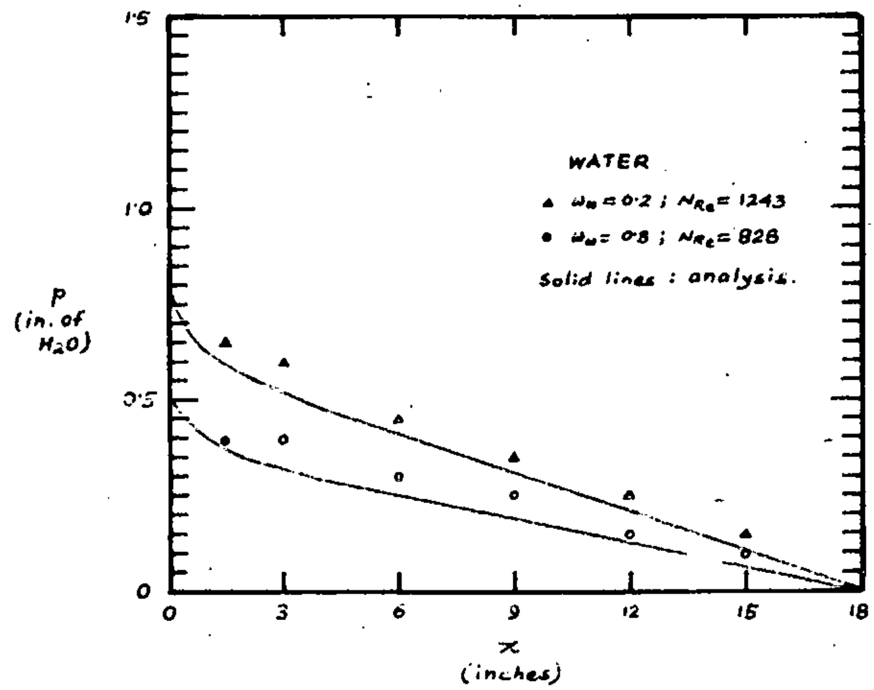
WATER
$\omega_w = 0{\cdot}2$; $N_{Re} = 1243$
$\omega_w = 0{\cdot}8$; $N_{Re} = 828$
Solid lines : analysis.
p (in. of H_2O)
x (inches)

Fig. 6

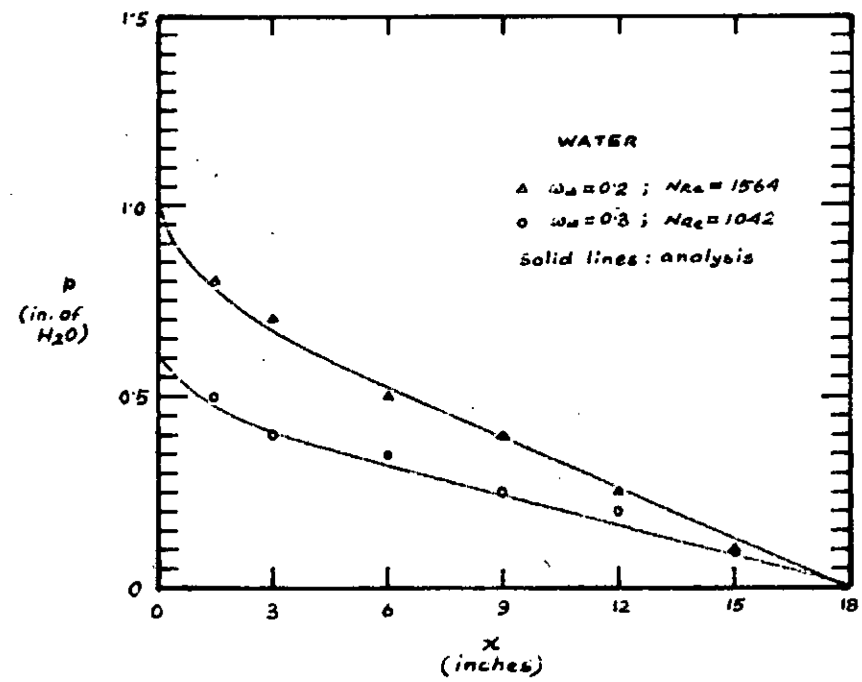
WATER
$\omega_w = 0{\cdot}2$; $N_{Re} = 1564$
$\omega_w = 0{\cdot}3$; $N_{Re} = 1042$
Solid lines : analysis
p (in. of H_2O)
x (inches)

Fig. 7

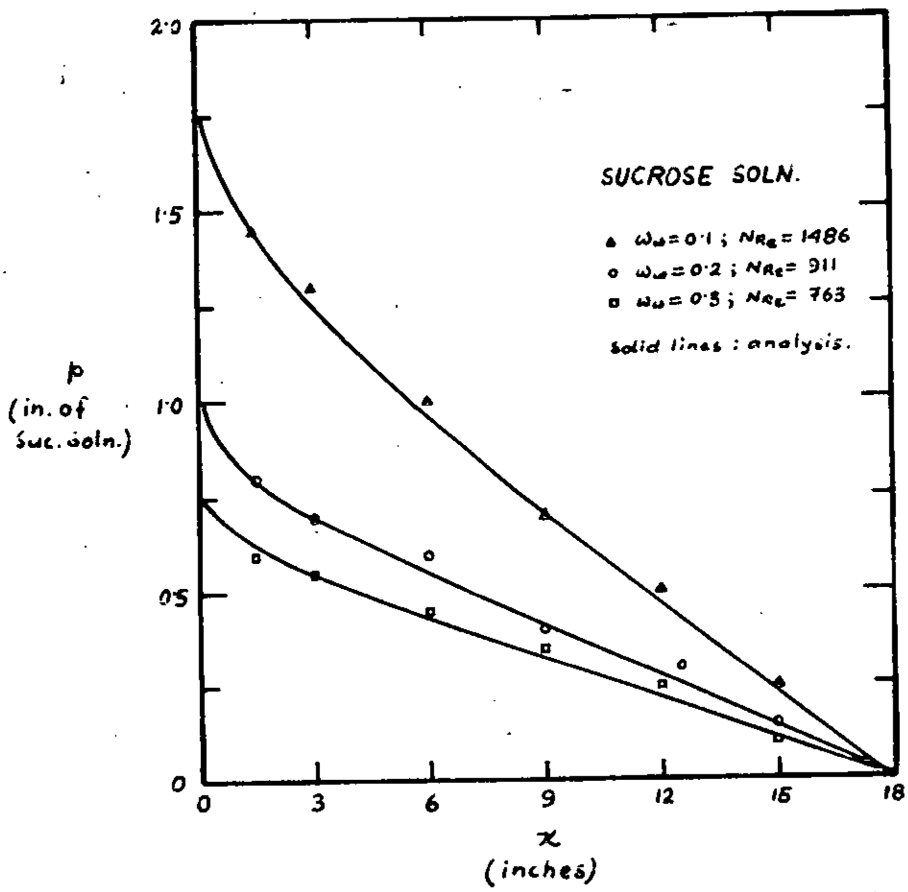
SUCROSE SOLN.
▲ $\omega_w = 0{\cdot}1$; $N_{Re} = 1486$
○ $\omega_w = 0{\cdot}2$; $N_{Re} = 911$
□ $\omega_w = 0{\cdot}3$; $N_{Re} = 763$
solid lines : analysis.
p
(in. of Suc. soln.)
2·0
1·5
1·0
0·5
0
0
3
6
9
12
15
18
x
(inches)

Fig. 8

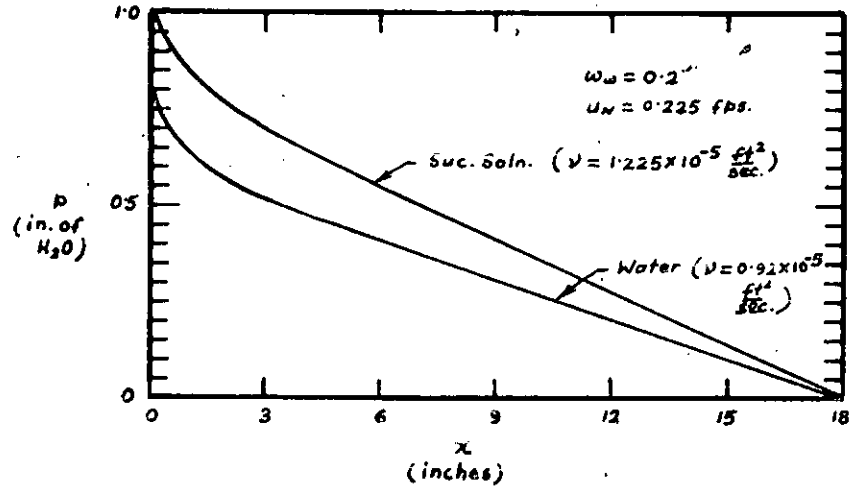
1·0
0·5
0
p
(in. of
H_2O)
$\omega_\omega = 0{\cdot}2''$
$u_N = 0{\cdot}225$ fps.
Suc. Soln. ($\nu = 1{\cdot}225 \times 10^{-5}\ \frac{ft^2}{sec.}$)
Water ($\nu = 0{\cdot}92 \times 10^{-5}\ \frac{ft^2}{sec.}$)
0
3
6
9
12
15
18
x
(inches)

Fig. 9

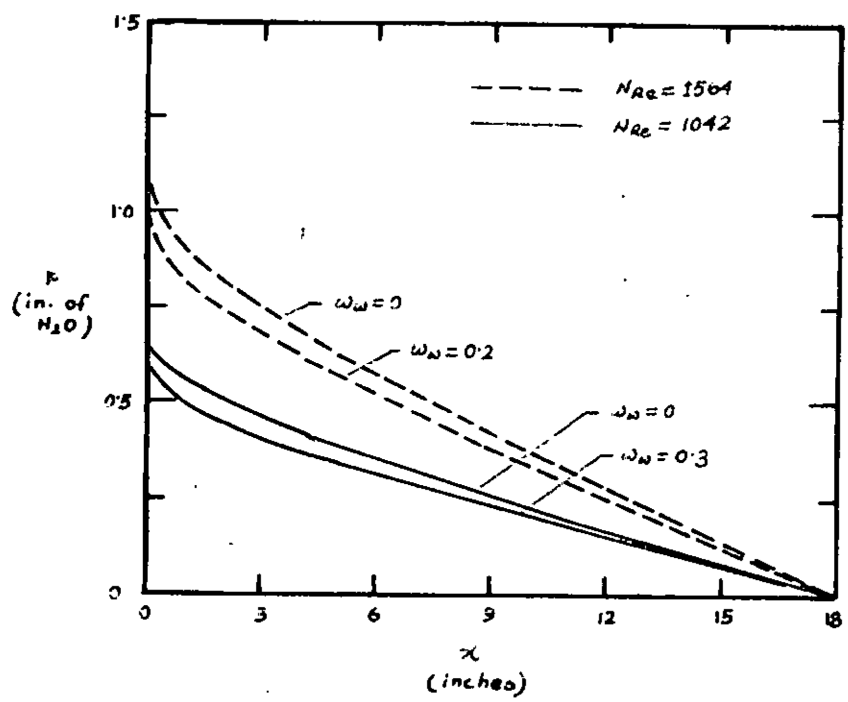
1·5
1·0
0·5
0
p
(in. of
H_2O)
$N_{Re} = 1564$
$N_{Re} = 1042$
$\omega_\omega = 0$
$\omega_\omega = 0{\cdot}2$
$\omega_\omega = 0$
$\omega_\omega = 0{\cdot}3$
0
3
6
9
12
15
18
x
(inches)

Fig. 10

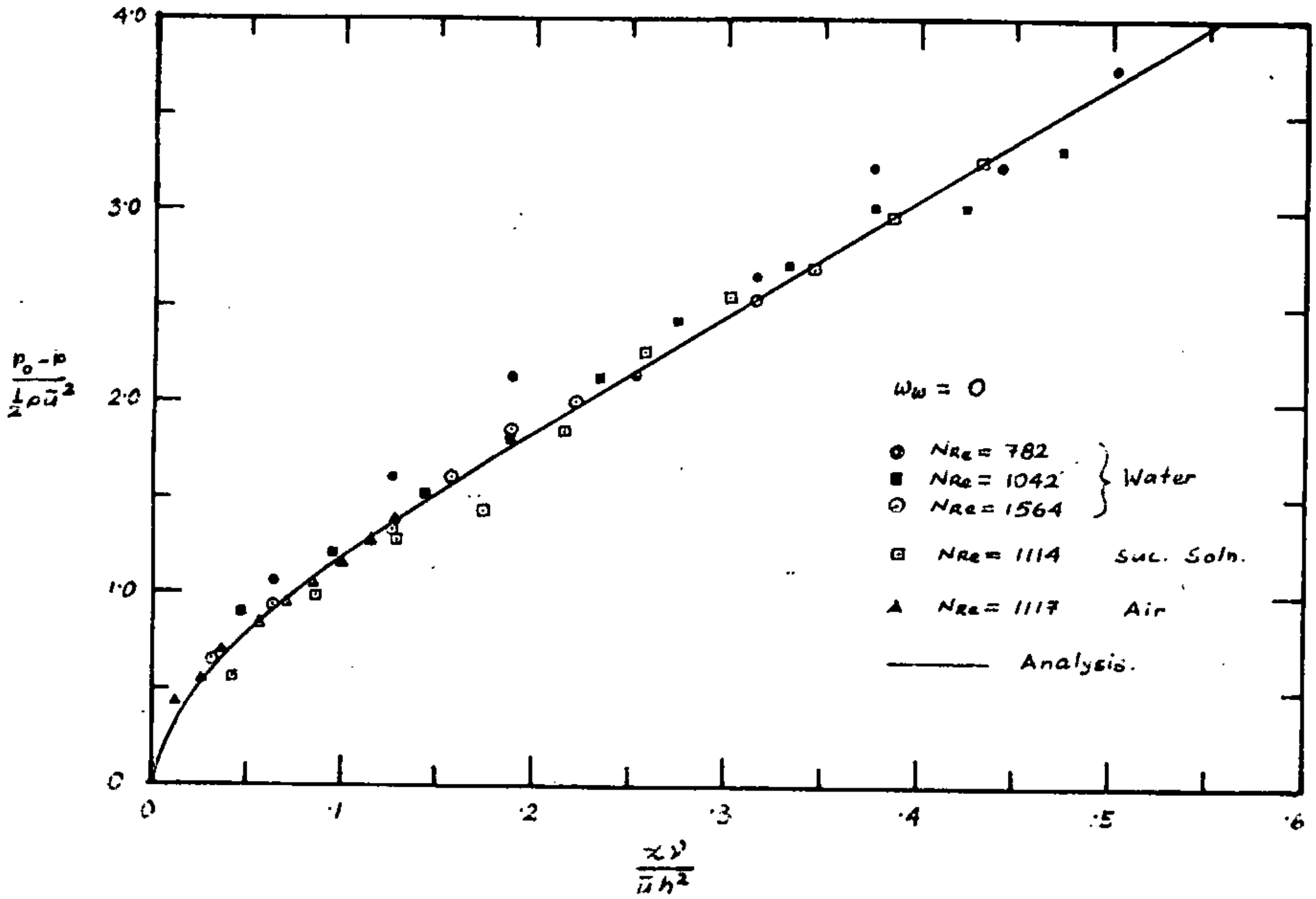
4·0
3·0
2·0
1·0
0
0
·1
·2
·3
·4
·5
·6
$\frac{p_o - p}{\frac{1}{2}\rho\bar{u}^2}$
$\frac{x\nu}{\bar{u}h^2}$
$\omega_w = 0$
$N_{Re} = 782$
$N_{Re} = 1042$
$N_{Re} = 1564$
Water
$N_{Re} = 1114$ Suc. Soln.
$N_{Re} = 1117$ Air
Analysis.

Fig. 11

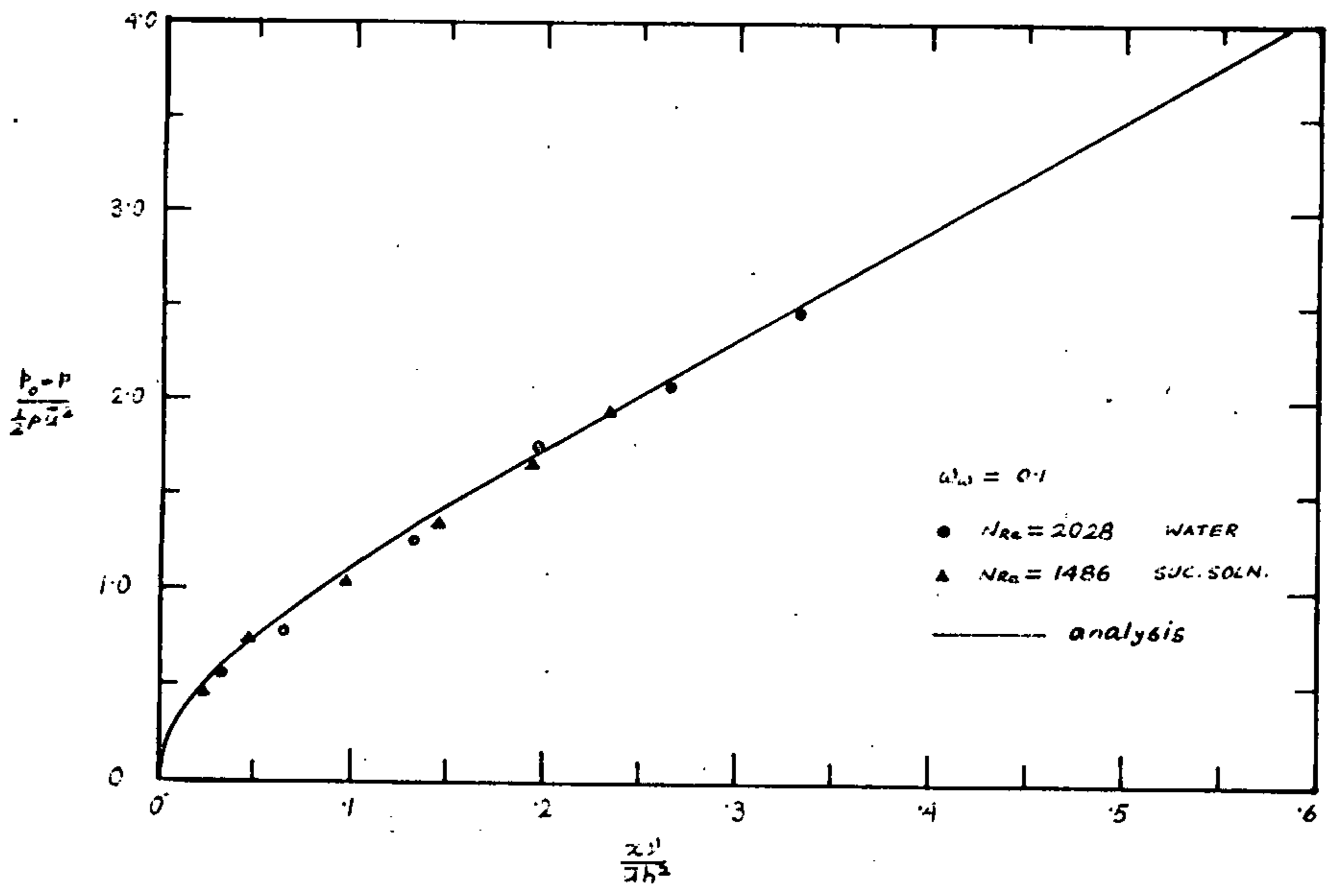
4·0
3·0
2·0
1·0
0
0
·1
·2
·3
·4
·5
·6
$\frac{p_o - p}{\frac{1}{2}\rho\bar{u}^2}$
$\frac{x\nu}{\bar{u}h^2}$
$\omega_w = 0{\cdot}1$
$N_{Re} = 2028$ WATER
$N_{Re} = 1486$ SUC. SOLN.
analysis

Fig. 12

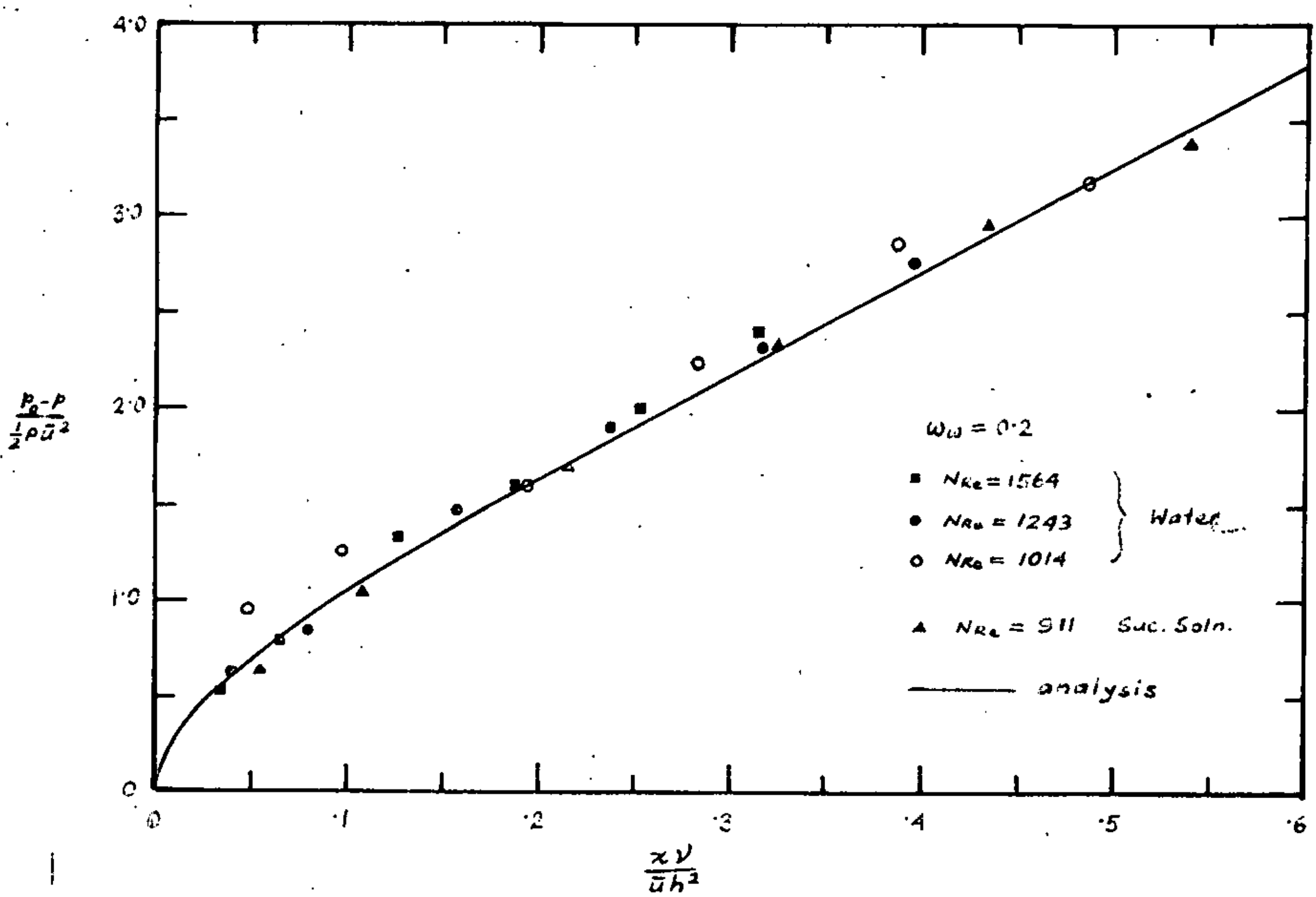

4·0
3·0
2·0
1·0
0
$\frac{p_0 - p}{\frac{1}{2}\rho \bar{u}^2}$
0
·1
·2
·3
·4
·5
·6
$\frac{x\nu}{\bar{u}h^2}$
$\omega_\omega = 0{\cdot}2$
$N_{Re} = 1564$
$N_{Re} = 1243$
$N_{Re} = 1014$
Water
$N_{Re} = 911$ Suc. Soln.
analysis

Fig. 13

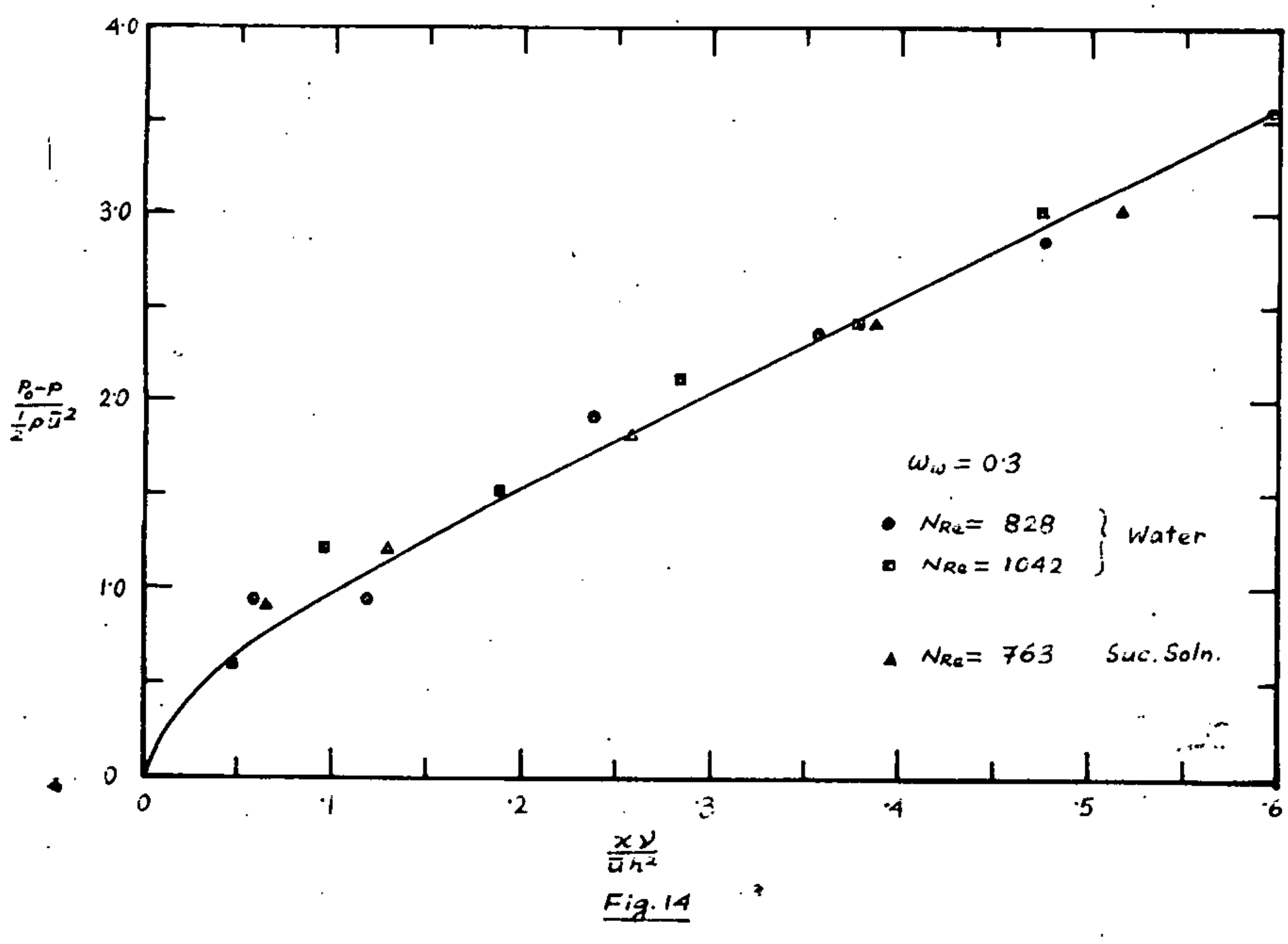

4·0
3·0
2·0
1·0
0
$\frac{p_0 - p}{\frac{1}{2}\rho \bar{u}^2}$
0
·1
·2
·3
·4
·5
·6
$\frac{x\nu}{\bar{u}h^2}$
$\omega_\omega = 0{\cdot}3$
$N_{Re} = 828$
$N_{Re} = 1042$
Water
$N_{Re} = 763$ Suc. Soln.

Fig. 14

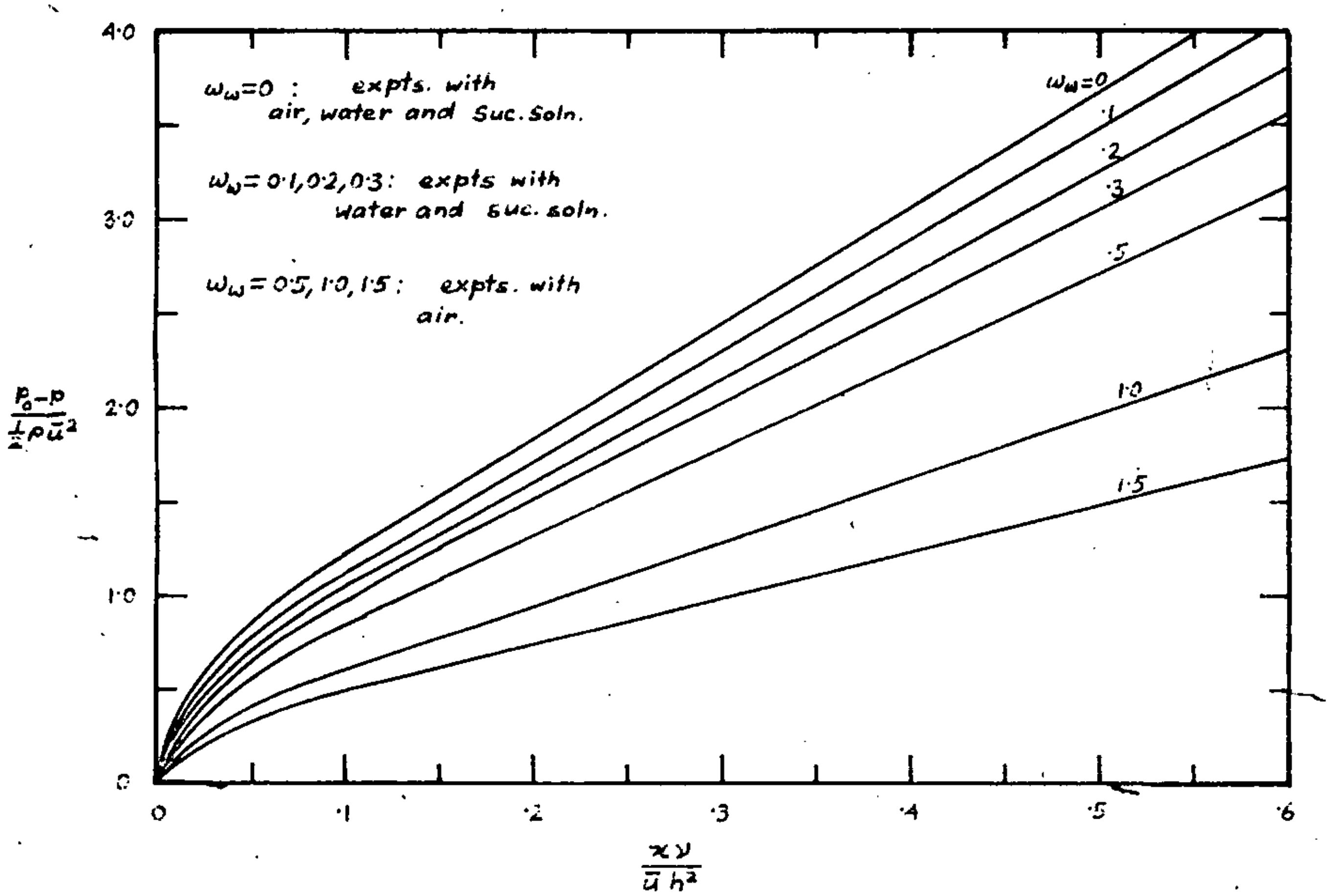

$\omega_\omega = 0$: expts. with air, water and Suc. Soln.
$\omega_\omega = 0{\cdot}1, 0{\cdot}2, 0{\cdot}3$: expts with water and suc. soln.
$\omega_\omega = 0{\cdot}5, 1{\cdot}0, 1{\cdot}5$: expts. with air.
$\omega_\omega = 0$
·1
·2
·3
·5
1·0
1·5
4·0
3·0
2·0
1·0
0
$\frac{p_0 - p}{\frac{1}{2}\rho \bar{u}^2}$
0
·1
·2
·3
·4
·5
·6
$\frac{x\nu}{\bar{u} h^2}$

Fig. 15

CHAPTER VI

CONCLUSIONS

The findings of this work lend strong support to the analytical model proposed and worked out by Sparrow and co-workers using the linearization technique for flow in a parallel-plate channel with one moving wall. The pressure field predictions stemming from this analysis were well supported by experimental results found in this project.

It is evident from the results of this investigation and the experiments done by Sparrow and Yu, that the theory is applicable for any fluid, liquid or gaseous, flowing through ducts. No deviations or anomalies from the analytical solutions were observed in the results of experiments with different fluids. The slight deviations of the results of the experiments were well within the accuracy of the experimental set-up.

It is therefore established that the original assumptions in linearizing the inertia terms of the momentum equation and the subsequent developments of the theory are justified. It has also been demonstrated that the equations of pressure vs. axial distance in the developed region derived by the linearization technique is exactly same as that obtained from basic equations of motion for Couette flow. The analytical method proposed and worked out by Sparrow and Yu covers both the developing and the developed regions and it can be concluded that it is a nice tool for predicting the velocity and pressure in the entire length of a channel flow.

The plot of dimensionless pressure vs. dimensionless axial distance at different values of the parameter " $u_w / \bar{u}$ " holds good for any fluid and it can be used to predict pressure distribution in flow through a similar configuration.

Ferther works in the field may be done for experimenting at very high and very low values of " $u_w / \bar{u}$ " which needs to design a different set-up for that purpose. It would also be interesting to carry out experiments in a inclined channel to include the effect of gravitation. Experiments for finding the entrance region lengths from the leading edge of ducts at different flow conditions may also be carried out. Determination of such lengths may be helpful for many practical purposes.

APPENDIX

Detailed mathematical steps of the theory in Chapter III

App. III(1)

$$\frac{\partial u}{\partial x} = \frac{\partial \omega}{\partial x}\cdot\frac{\partial u}{\partial \omega} = \frac{\partial \omega}{\partial x^*}\,\frac{\partial x^*}{\epsilon\,\partial x^*}\,\frac{\partial u}{\partial \omega}$$

$$= \frac{\partial \omega}{\partial x^*}\,\frac{1}{\epsilon}\,\frac{\nu}{\bar{u}h^2}\,\bar{u} = \frac{\nu}{\epsilon h^2}\,\frac{\partial \omega}{\partial x^*}$$

$$\frac{\partial u}{\partial y} = \frac{\partial \omega}{\partial \eta}\,\frac{\partial \eta}{\partial y}\,\frac{\partial u}{\partial \omega} = \frac{\bar{u}}{h}\,\frac{\partial \omega}{\partial \eta}$$

$$\frac{\partial^2 u}{\partial y^2} = \frac{\partial}{\partial y}\left(\frac{\partial u}{\partial y}\right) = \frac{\bar{u}}{h}\,\frac{\partial \eta}{\partial y}\,\frac{\partial}{\partial \eta}\left(\frac{\partial \omega}{\partial \eta}\right) = \frac{\bar{u}}{h^2}\,\frac{\partial^2 \omega}{\partial \eta^2}$$

again, at $y = h$, $\eta = +1$ and $y = -h$, $\eta = -1$
Substitution of these values in eqn.7 yields eqn. 8.

App. III(2)

Integrating once, eqn.10 yields,

$$\frac{\partial \omega}{\partial \eta} = \frac{1}{2}\left[\left(\frac{\partial \omega}{\partial \eta}\right)_1 - \left(\frac{\partial \omega}{\partial \eta}\right)_{-1}\right]\eta + c_1$$

$$\therefore\; c_1 = \frac{1}{2}\left[\left(\frac{\partial \omega}{\partial \eta}\right)_1 + \left(\frac{\partial \omega}{\partial \eta}\right)_{-1}\right]$$

$$\frac{\partial \omega}{\partial \eta} = \frac{1}{2}\left[\left(\frac{\partial \omega}{\partial \eta}\right)_1 - \left(\frac{\partial \omega}{\partial \eta}\right)_{-1}\right]\eta + \frac{1}{2}\left[\left(\frac{\partial \omega}{\partial \eta}\right)_1 + \left(\frac{\partial \omega}{\partial \eta}\right)_{-1}\right]$$

Integrating again with respect to η,

$$\omega = \frac{1}{4}\left[\left(\frac{\partial \omega}{\partial \eta}\right)_1 - \left(\frac{\partial \omega}{\partial \eta}\right)_{-1}\right]\eta^2 + \frac{1}{2}\left[\left(\frac{\partial \omega}{\partial \eta}\right)_1 + \left(\frac{\partial \omega}{\partial \eta}\right)_{-1}\right]\eta + c_2$$

$\omega = 0$ at $\eta = +1$ gives,

$$c_2 = -\left[\frac{3}{4}\left(\frac{\partial \omega}{\partial \eta}\right)_1 + \frac{1}{4}\left(\frac{\partial \omega}{\partial \eta}\right)_{-1}\right]$$

$$\therefore\; \omega = \frac{1}{4}\left[\left(\frac{\partial \omega}{\partial \eta}\right)_1 - \left(\frac{\partial \omega}{\partial \eta}\right)_{-1}\right]\eta^2 + \frac{1}{2}\left[\left(\frac{\partial \omega}{\partial \eta}\right)_1 + \left(\frac{\partial \omega}{\partial \eta}\right)_{-1}\right]\eta - \left[\frac{3}{4}\left(\frac{\partial \omega}{\partial \eta}\right)_1 + \frac{1}{4}\left(\frac{\partial \omega}{\partial \eta}\right)_{-1}\right]$$

App. III(3)
$$\frac{1}{2}\int_{-1}^{1}\omega\,d\eta = 1$$

$$\therefore \frac{1}{2}\left\{\frac{1}{12}\left[\left(\frac{\partial\omega}{\partial\eta}\right)_1-\left(\frac{\partial\omega}{\partial\eta}\right)_{-1}\right]\eta^3+\frac{1}{4}\left[\left(\frac{\partial\omega}{\partial\eta}\right)_1+\left(\frac{\partial\omega}{\partial\eta}\right)_{-1}\right]\eta - \left[\frac{3}{4}\left(\frac{\partial\omega}{\partial\eta}\right)_1+\frac{1}{4}\left(\frac{\partial\omega}{\partial\eta}\right)_{-1}\right]\right\}_{-1}^{+1} = 1$$

$$\text{or,}\quad 2\left(\frac{\partial\omega}{\partial\eta}\right)_1+\left(\frac{\partial\omega}{\partial\eta}\right)_{-1} = -3$$

App. III(4)

$$g''+\lambda^2 g = \frac{1}{2}\left[g'(1)-g'(-1)\right]$$

For complimentary solution we put,

$$g''+\lambda^2 g = 0 \qquad \text{whence,}$$

$$g = A\cos\lambda\eta + B\sin\lambda\eta$$

For particular solution we use operator "D" and write the "g" eqn. as

$$D^2 g + \lambda^2 g = \frac{1}{2}K \qquad \left\{ K = \left[g'(1)-g'(-1)\right]\right.$$

$$\therefore\ g = \frac{1}{2}K\frac{1}{\lambda^2}\left[1-\frac{D^2}{\lambda^2}\right]^{-1} = \frac{K}{2\lambda^2}\left[1-\frac{D^2}{\lambda^2}+\cdots\cdots\right]$$

$$= \frac{K}{2\lambda^2}$$

Therefore General solution is,

$$g = A\cos\lambda\eta + B\sin\lambda\eta + \frac{1}{2\lambda^2}\left[g'(1)-g'(-1)\right]$$

App. III(5)

$$g = A\left[\cos\lambda\eta-\cos\lambda\right] = -A\cos\lambda\left[1-\frac{\cos\lambda\eta}{\cos\lambda}\right]$$

$$= -A\left[1-\frac{\cos\lambda\eta}{\cos\lambda}\right] \qquad \left[\text{since } \lambda\to 0\right]$$

Writing eqn. of g for all values of λ and replacing α for λ and inserting $\frac{1}{\alpha_m}$ for a constant in order to normalize g, one gets,

$$g_m = \frac{1}{\alpha_m}\left[1 - \frac{\cos\alpha_m\eta}{\cos\alpha_m}\right], \qquad m = 1, 2, 3 \ldots\ldots$$

App. III(6)(a)

$$\int_{-1}^{1} G_n^2 d\eta = \int_{-1}^{1} \sin^2 n\pi\eta \, d\eta = \frac{1}{2}\int_{-1}^{1}\left[1 - \cos 2n\pi\eta\right] d\eta$$
$$= \frac{1}{2}\left[\eta - \frac{\sin 2n\pi\eta}{2n\pi}\right]_{-1}^{+1} = \frac{1}{2}\times 2 = 1$$

App. III(6)(b)

$$\int_{-1}^{1} g_m^2 d\eta = \frac{1}{\alpha_m^2}\int_{-1}^{+1}\left[1 - \frac{\cos\alpha_m\eta}{\cos\alpha_m}\right]^2 d\eta$$
$$= \frac{1}{\alpha_m^2}\int_{-1}^{+1}\left[1 - 2\,\frac{\cos\alpha_m\eta}{\cos\alpha_m} + \frac{\frac{1}{2}\{1 + \cos 2\alpha_m\eta\}}{\cos^2\alpha_m}\right] d\eta$$
$$= \frac{1}{\alpha_m^2}\left[\eta - 2\,\frac{\sin\alpha_m\eta}{\alpha_m\cos\alpha_m} + \frac{\eta + \frac{\sin 2\alpha_m\eta}{2\alpha_m}}{2\cos^2\alpha_m}\right]_{-1}^{+1}$$
$$= \frac{1}{\alpha_m^2}\left[2 - 4\,\frac{\tan\alpha_m}{\alpha_m} + \frac{2}{2\cos^2\alpha_m} + \frac{4\sin\alpha_m\cos\alpha_m}{4\alpha_m\cos^2\alpha_m}\right]$$
$$= \frac{1}{\alpha_m^2}\left[2 - 4 + \frac{1}{\cos^2\alpha_m} + \frac{\tan\alpha_m}{\alpha_m}\right] = \frac{1}{\alpha_m^2}\left[-1 + \frac{1}{\cos^2\alpha_m}\right]$$
$$= \frac{1 - \cos^2\alpha_m}{\cos^2\alpha_m} \times \frac{1}{\alpha_m^2} = \frac{\tan^2\alpha_m}{\alpha_m^2} = 1$$

App. III(7)(a)

$$\int_{-1}^{1} g_m G_n d\eta = \int_{-1}^{1}\frac{1}{\alpha_m}\left[1 - \frac{\cos\alpha_m\eta}{\cos\alpha_m}\right]\sin n\pi\eta \, d\eta$$
$$= \int_{-1}^{1}\frac{1}{\alpha_m}\left[\sin n\pi\eta - \frac{\sin n\pi\eta \cos\alpha_m\eta}{\cos\alpha_m}\right] d\eta$$

$$= \frac{1}{\alpha_m}\left[-\frac{\cos n\pi\eta}{n\pi}\right]_{-1}^{1} - \frac{1}{\cos\alpha_m}\int_{-1}^{1}\frac{1}{2}\left[\sin(n\pi+\alpha_m)\eta + \sin(n\pi-\alpha_m)\eta\right]d\eta$$

$$= 0 - \frac{1}{2\cos\alpha_m}\left[-\frac{\cos(n\pi+\alpha_m)\eta}{(n\pi+\alpha_m)} - \frac{\cos(n\pi-\alpha_m)\eta}{(n\pi-\alpha_m)}\right]_{-1}^{+1}$$

$$= 0$$

App. III (7)(b) $\qquad \int_{-1}^{1} g_m g_i \, d\eta$

$$= \frac{1}{\alpha_m\alpha_i}\int_{-1}^{1}\left[\left(1-\frac{\cos\alpha_m\eta}{\cos\alpha_m}\right)\left(1-\frac{\cos\alpha_i\eta}{\cos\alpha_i}\right)\right]d\eta$$

$$= \frac{1}{\alpha_m\alpha_i}\int_{-1}^{1}\left[1 - \frac{\cos\alpha_i\eta}{\cos\alpha_i} - \frac{\cos\alpha_m\eta}{\cos\alpha_m} + \frac{\frac{1}{2}\left\{\cos(\alpha_m+\alpha_i)\eta + \cos(\alpha_m-\alpha_i)\eta\right\}}{\cos\alpha_m\cos\alpha_i}\right]d\eta$$

$$= \frac{1}{\alpha_m\alpha_i}\left[\eta - \frac{\sin\alpha_i\eta}{\alpha_i\cos\alpha_i} - \frac{\sin\alpha_m\eta}{\alpha_m\cos\alpha_m} + \frac{\frac{\sin(\alpha_m+\alpha_i)\eta}{(\alpha_m+\alpha_i)} + \frac{\sin(\alpha_m-\alpha_i)\eta}{(\alpha_m-\alpha_i)}}{2\cos\alpha_m\cos\alpha_i}\right]_{-1}^{1}$$

$$= \frac{1}{\alpha_m\alpha_i}\left[2 - 2 - 2 + \frac{2+2}{2\cos\alpha_m\cos\alpha_i}\right] = \frac{1}{\alpha_m\alpha_i}\left[2-2-2+2\right] = 0$$

App. III (7)(c) $\qquad \int_{-1}^{1} G_n G_j \, d\eta = \int_{-1}^{1}\sin n\pi\eta \sin j\pi\eta \, d\eta$

$$= \int_{-1}^{1}\frac{1}{2}\left[\sin(n\pi+j\pi)\eta + \sin(n\pi-j\pi)\eta\right]d\eta$$

$$= \frac{1}{2}\left[-\frac{\cos(n+j)\pi\eta}{(n+j)\pi} - \frac{\cos(n-j)\pi\eta}{(n-j)\pi}\right]_{-1}^{+1} = \frac{1}{2}\times\left[0-0\right] = 0$$

App. III (8)(a)

$$\omega_0(\eta) = \omega_{fd}(\eta) + \sum_{m=1}^{\infty} C_m g_m(\eta) + \sum_{n=1}^{\infty} D_n G_n(\eta)$$

$$\therefore \quad \underbrace{\omega_0(\eta)\, g_i(\eta)}_{(iv)} = \underbrace{\omega_{fd}(\eta)\, g_i(\eta)}_{(iii)} + \underbrace{\sum_{m=1}^{\infty} C_m g_m(\eta) g_i(\eta)}_{(ii)} + \underbrace{\sum_{n=1}^{\infty} D_n G_n(\eta)\, g_i(\eta)}_{(i)}$$

Now, integration with respect to η between the limits -1 to $+1$ is performed :

(i) $\displaystyle\int_{-1}^{1} D_n G_n(\eta) g_i(\eta)\, d\eta = 0$ according to 28(b)

(ii) $\displaystyle\int_{-1}^{1} \left[\sum_{m=1}^{\infty} C_m g_m(\eta) g_i(\eta)\right] d\eta$

$\displaystyle = \int_{-1}^{1} C_i\, g_i^{2}(\eta)\, d\eta$ [all other terms in the expansion becomes zero according to 28(a)]

$= C_i$

(iii) $\displaystyle\int_{-1}^{1} w_{fd}(\eta)\, g_i(\eta)\, d\eta$

$$= \int_{-1}^{1} \frac{1}{\alpha_i}\left[\frac{3}{4}(w_w-2)\eta^2 - \frac{1}{2} w_w \eta + \frac{3}{2} - \frac{1}{4} w_w\right]\left[1 - \frac{\cos\alpha_i\eta}{\cos\alpha_i}\right] d\eta$$

$$= \frac{1}{\alpha_i}\left[\frac{1}{4}(w_w-2)\eta^3 - \frac{1}{4} w_w \eta^2 + \frac{3}{2}\eta - \frac{1}{4} w_w \eta\right]_{-1}^{1}$$

$$- \frac{1}{\alpha_i}\left[\frac{3}{4}(w_w-2)\int_{-1}^{1}\frac{\eta^2\cos\alpha_i\eta}{\cos\alpha_i}\, d\eta - \frac{1}{2} w_w \int_{-1}^{1}\frac{\eta\cos\alpha_i\eta}{\cos\alpha_i}\, d\eta \right.$$

$$\left. + \frac{3}{2}\int_{-1}^{1}\frac{\cos\alpha_i\eta}{\cos\alpha_i}\, d\eta - \frac{1}{4} w_w \int_{-1}^{1}\frac{\cos\alpha_i\eta}{\cos\alpha_i}\, d\eta\right]$$

$$= \frac{1}{\alpha_i}\left[\frac{w_w-2}{2} + 3 - \frac{1}{2} w_w\right]$$

$$- \frac{1}{\alpha_i}\left[\frac{3}{4}\frac{(w_w-2)}{\cos\alpha_i}\int_{-1}^{1}\frac{(\alpha_i\eta)^2\cos\alpha_i\eta\, d(\alpha_i\eta)}{\alpha_i^{3}}\right.$$

$$- \frac{w_w}{2\cos\alpha_i}\int_{-1}^{1}\frac{(\alpha_i\eta)\cos(\alpha_i\eta)\, d(\alpha_i\eta)}{\alpha_i^{2}}$$

$$\left. + \frac{3}{2\cos\alpha_i}\int_{-1}^{1}\cos\alpha_i\eta\, d\eta - \frac{w_w}{4\cos\alpha_i}\int_{-1}^{1}\cos\alpha_i\eta\, d\eta\right]$$

$$= \frac{1}{\alpha_i}(2) - \frac{1}{\alpha_i}\Big[\frac{3}{4}\frac{(\omega_w-2)}{\alpha_i^3\cos\alpha_i}\Big\{2\alpha_i\eta\cos\alpha_i\eta+(\alpha_i^2\eta^2-2)\sin\alpha_i\eta\Big\}$$

$$-\frac{\omega_w}{2\cos\alpha_i}\Big\{\cos\alpha_i\eta+\alpha_i\eta\sin\alpha_i\eta\Big\} + \frac{3}{2\cos\alpha_i}\frac{\sin\alpha_i\eta}{\alpha_i}$$

$$-\frac{\omega_w}{4\cos\alpha_i}\frac{\sin\alpha_i\eta}{\alpha_i}\Big]_{-1}^{+1}$$

[C.R.C. Integration table is used]

$$= \frac{2}{\alpha_i} - \frac{1}{\alpha_i}\Big[\frac{3}{4}\frac{\omega_w-2}{\alpha_i^3\cos\alpha_i}\Big\{4\alpha_i\cos\alpha_i+2\alpha_i^2\sin\alpha_i-4\sin\alpha_i\Big\}$$

$$-\frac{\omega_w}{2\cos\alpha_i}\Big\{0\Big\} + \frac{3\sin\alpha_i}{\alpha_i\cos\alpha_i} - \frac{\omega_w}{2\alpha_i\cos\alpha_i}\sin\alpha_i\Big]$$

$$= \frac{2}{\alpha_i} - \frac{1}{\alpha_i}\Big[\frac{3(\omega_w-2)}{\alpha_i^2} + \frac{3}{2}\frac{(\omega_w-2)}{\alpha_i}\tan\alpha_i - \frac{3(\omega_w-2)}{\alpha_i^3}\tan\alpha_i$$

$$+\frac{3\tan\alpha_i}{\alpha_i} - \frac{1}{2}\omega_w\frac{\tan\alpha_i}{\alpha_i}\Big]$$

$$= \frac{2}{\alpha_i} - \frac{1}{\alpha_i}\Big[\frac{3}{2}(\omega_w-2)+3-\frac{1}{2}\omega_w\Big]$$

$$= \frac{2}{\alpha_i} - \frac{1}{\alpha_i}\big[\omega_w\big]$$

(iv) $$\int_{-1}^{1}\frac{\omega_o(\eta)}{\alpha_i}\Big(1-\frac{\cos\alpha_i\eta}{\cos\alpha_i}\Big)d\eta$$

$$= \int_{-1}^{1}\frac{\omega_o(\eta)}{\alpha_i}d\eta - \frac{1}{\alpha_i}\int_{-1}^{1}\omega_o(\eta)\frac{\cos\alpha_i\eta}{\cos\alpha_i}d\eta$$

Now, combining (i), (ii), (iii) & (iv) and writing m for i to generalize,

$$c_m = \int_{-1}^{1}\frac{\omega_o(\eta)}{\alpha_m}d\eta - \frac{2}{\alpha_m} + \frac{1}{\alpha_m}\Big[\omega_w - \int_{-1}^{1}\omega_o(\eta)\frac{\cos\alpha_m\eta}{\cos\alpha_m}d\eta\Big].$$

$$\underbrace{w_o(\eta)G_j(\eta)}_{(iv)} = \underbrace{w_{fd}(\eta)G_j(\eta)}_{(iii)} + \underbrace{\sum_{m=1}^{\infty} C_m g_m(\eta)G_j(\eta)}_{(i)} + \underbrace{\sum_{n=1}^{\infty} D_n G_n(\eta)G_j(\eta)}_{(ii)}$$

Integration between the limits -1 to $+1$ is now performed:

(i) $\displaystyle\sum_{m=1}^{\infty}\int_{-1}^{1} C_m g_m G_j \, d\eta = 0$ according to 28(b)

(ii) $\displaystyle\sum_{n=1}^{\infty}\int_{-1}^{1} D_n G_n G_j \, d\eta = D_j\int_{-1}^{1} G_j^2 \, d\eta = D_j$

(iii) $\displaystyle\int_{-1}^{1}\left[\frac{3}{4}(w_w-2)\eta^2 - \frac{1}{2}w_w\eta + \frac{3}{2} - \frac{1}{4}w_w\right]\sin j\pi\eta \, d\eta$

$$= \frac{3}{4}(w_w-2)\frac{1}{(j\pi)^3}\int_{-1}^{1}(j\pi\eta)^2\sin(j\pi\eta)\,d(j\pi\eta)$$

$$-\frac{1}{2}w_w\frac{1}{(j\pi)^2}\int_{-1}^{1}(j\pi\eta)\sin(j\pi\eta)\,d(j\pi\eta) + \frac{3}{2}\int_{-1}^{1}\sin(j\pi\eta)\,d\eta$$

$$-\frac{1}{4}w_w\int_{-1}^{1}\sin(j\pi\eta)\,d\eta$$

$$= \frac{3}{4}\frac{(w_w-2)}{(j\pi)^3}\left[2j\pi\eta\sin j\pi\eta - \{(j\pi\eta)^2-2\}\cos j\pi\eta\right]_{-1}^{1}$$

$$-\frac{w_w}{2(j\pi)^2}\left[\sin(j\pi\eta) - (j\pi\eta)\cos(j\pi\eta)\right]_{-1}^{+1}$$

$$-\frac{3}{2}\left[\frac{\cos j\pi\eta}{j\pi}\right]_{-1}^{1} + \frac{1}{4}w_w\left[\frac{\cos j\pi\eta}{j\pi}\right]_{-1}^{+1}$$

[Ref. CRC Integration table p 296]

$$= -\frac{w_w}{2(j\pi)^2}\left[2\sin(j\pi) - 2j\pi\cos(j\pi)\right]$$

$$= \frac{w_w}{j\pi}\cos(j\pi) = \frac{(-1)^j}{j\pi}w_w$$

(iv) $$\int_{-1}^{1} \omega_0(\eta)\, G_j(\eta)\, d\eta = \int_{-1}^{1} \omega_0(\eta) \sin j\pi\eta \, d\eta$$

Now combining (i), (ii), (iii) & (iv) and writing n for j to generalize,

$$D_n = -\frac{(-1)^n}{n\pi}\,\omega_\omega + \int_{-1}^{1} \omega_0(\eta) \sin n\pi\eta \, d\eta$$

App. III (9) $$\frac{\partial}{\partial x}(u^2) + \frac{\partial}{\partial y}(uv) = -\frac{1}{\rho}\frac{dp}{dx} + \nu \frac{\partial^2 u}{\partial y^2}$$

Integrating w.r.t. y between the limits $-h$ to $+h$,

$$\frac{d}{dx}\int_{-h}^{h} u^2 \partial y + uv\Big]_{-h}^{+h} = -\frac{1}{\rho}\frac{dp}{dx}\,2h + \nu\left[\left(\frac{\partial u}{\partial y}\right)_h - \left(\frac{\partial u}{\partial y}\right)_{-h}\right]$$

or, $$\frac{d}{dx}\int_{-1}^{1} \omega^2 d\eta \;\frac{h.\nu.\bar{u}^2}{\bar{u}\,h^2} = -\frac{1}{\rho}\,2h\,\frac{\nu}{\bar{u}h^2}\,\frac{dp}{dx} + \nu\frac{\bar{u}}{h}\left[\left(\frac{\partial \omega}{\partial \eta}\right)_1 - \left(\frac{\partial \omega}{\partial \eta}\right)_{-1}\right]$$

or, $$-\frac{1}{\rho\bar{u}^2}\frac{dp}{dx} = \frac{1}{2}\frac{d}{dx}\int_{-1}^{1}\omega^2 d\eta - \frac{1}{2}\left[\left(\frac{\partial \omega}{\partial \eta}\right)_1 - \left(\frac{\partial \omega}{\partial \eta}\right)_{-1}\right]$$

App. III (10) Integration of eqn. derived in App. III (9) w.r.t. X (between limits 0 to X) yields,

$$-\frac{1}{\rho\bar{u}^2}(p - p_0) = \left[\frac{1}{2}\int_{-1}^{1}\omega^2 d\eta\right]_{X=0}^{X=X} - \frac{1}{2}\int_0^X \left[\left(\frac{\partial \omega}{\partial \eta}\right)_1 - \left(\frac{\partial \omega}{\partial \eta}\right)_{-1}\right] dX$$

or, $$\frac{p_0 - p}{\frac{1}{2}\rho\bar{u}^2} = \int_{-1}^{1}\omega^2 d\eta - \int_{-1}^{1}\omega_0^2 d\eta - \frac{1}{2}\int_0^X \left\{\left(\frac{\partial \omega_{fd}}{\partial \eta}\right)_{-1}^{+1} + \left(\frac{\partial \omega^*}{\partial \eta}\right)_{-1}^{1}\right\} dX$$

$$[\omega = \omega_{fd} + \omega^*]$$

$$\text{or,} \quad \frac{p_0 - p}{\frac{1}{2}\rho\bar{u}^2} = \int_{-1}^{1} \omega^2 d\eta - \int_{-1}^{1} \omega_0^2 d\eta - \int_0^{x} \left[\left(\frac{\partial \omega^*}{\partial \eta}\right)_1 - \left(\frac{\partial \omega^*}{\partial \eta}\right)_{-1} \right] dx$$

$$- \int_0^{x} \left[\frac{3}{2}(\omega_\omega - 2)\eta - \frac{1}{2}\,\omega_\omega \right]_{-1}^{1} dx$$

$$\text{or,} \quad \frac{p_0 - p}{\frac{1}{2}\rho\bar{u}^2} = 3(2 - \omega_\omega)x + \int_{-1}^{1} \omega^2 d\eta - \int_{-1}^{1} \omega_0^2 d\eta$$

$$- \int_0^{x^*} \left[\left(\frac{\partial \omega^*}{\partial \eta}\right)_1 - \left(\frac{\partial \omega^*}{\partial \eta}\right)_{-1} \right] \epsilon\, dx^*$$

or, we can write,

$$\frac{p_0 - p}{\frac{1}{2}\rho\bar{u}^2} = \frac{(p_0 - p)_{fd}}{\frac{1}{2}\rho\bar{u}^2} + K(x)$$

where, $$\frac{(p_0 - p)_{fd}}{\frac{1}{2}\rho\bar{u}^2} = 3(2 - \omega_\omega)\frac{x\nu}{\bar{u}h^2}$$

and $$K(x) = \int_{-1}^{1} \omega^2 d\eta - \int_{-1}^{1} \omega_0^2 d\eta - \int_0^{x^*} \left[\left(\frac{\partial \omega^*}{\partial \eta}\right)_1 - \left(\frac{\partial \omega^*}{\partial \eta}\right)_{-1} \right] \epsilon\, dx^*$$

App. V-1

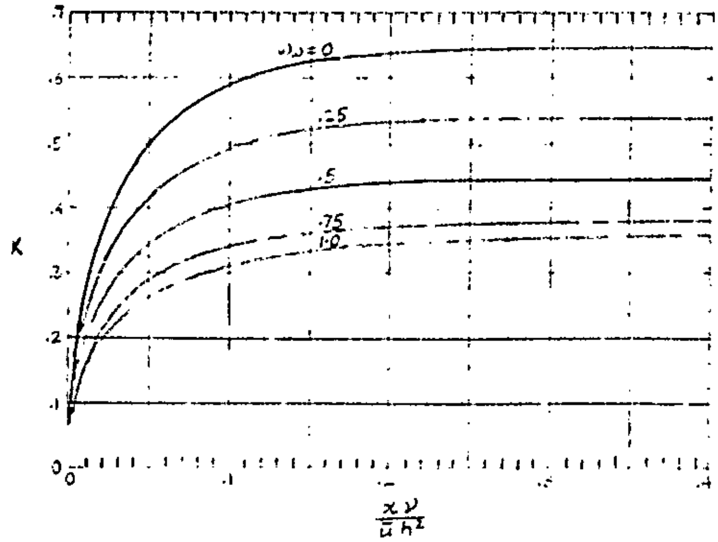

K(x) vs. $\frac{x\nu}{\bar{u}h^2}$, $0 \leq \omega_0 \leq 1$ (Ref. 2, [illegible])

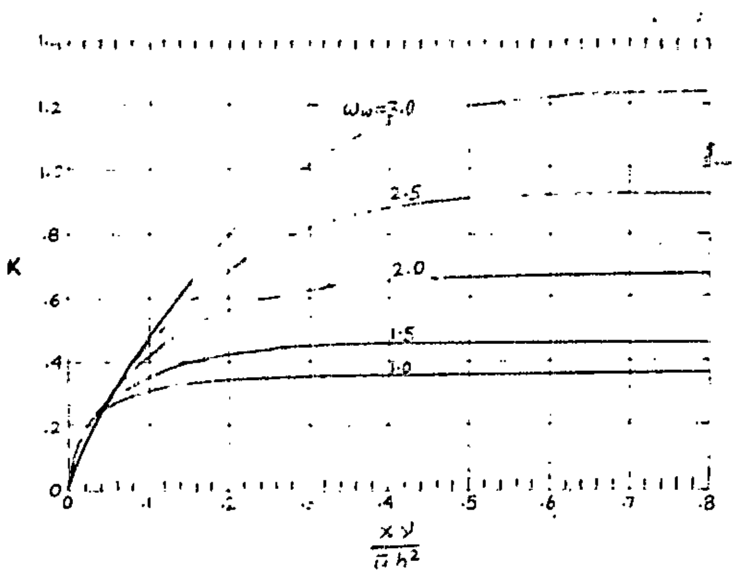

K [illegible] $1 \leq$ [illegible] 3 ([illegible] 2, [illegible])

App. V-2

OBSERVATION SHEET

	No. of obs.	Distance of taps from leading edge inches	0	1.5	3.0	4.5	6.0	7.5	9.0	10.5	12.0	13.5	15.0	Flow-rate : Wt. of liq. collected per 20 secs. lbs-ozs.	Wall Speed fpm.
Experiments with WATER Operating temp. = 81^oF = 62.2 lbs/ft^3 = $.92 \times 10^{-5}$ ft^2/sec.	1-1	Static Pressure in inches of Water.	.5	.4	.35	.3	.3	.25	.2	.2	.15	.1	.1	3 - 0	0
	1-2		.65	..5	.45	.4	.35	.3	.25	.2	.15	.15	.1	4 - 0	
	1-3		1.1	.85	.75	.65	.6	.5	.4	.35	.3	.2	.15	6 - 0	
	2-1		1.4	1.1	.95		.75		.55		.35		.2	7 - 12	11
	2-2		.6	.45	.4		.35		.25		.15		.1	3 - 14	
	3-1		.8	.65	.6		.45		.35		.25		.15	4 -12	13.5
	3-2		.5	.4	.4		.3		.25		.2		.1	3 - 2½	
	4-1		1.0	.8	.7		.5		.4		.25		.1	6 - 0	17
	4-2		.6	.5	.4		.35		.25		.2		.1	4 - 0	
Experiments with SUCROSE SOLN. Op. temp. = 65^oF = 64.15 lb/ft^3 = 1.255 ft^2/sec.	5-1	Static Pressure in inches of Suc. Soln.	1.35	1.15	1.0	.9	.75	.7	.55	.45	.4	.3	.2	6 - 0	0
	5-2		1.8	1.45	1.3		1.0		.7		.5		.25	8 - 0	11
	5-3		1.0	.8	.7		.6		.4		.3		.15	4 - 14½	13.5
	5-4		.75	.6	.55		.45		.35		.25		.1	4 - 1.8	17

App. V-3

RESULTS :

Obs No. 1-1	x	X	Analytical $\frac{p_o - p}{\frac{1}{2}\rho\bar{u}^2}$	p	p corrected for exit error.	Experimental $\frac{p_o - p}{\frac{1}{2}\rho\bar{u}^2}$
	1.5	.063	.918	.414	.399	1.070
	3.0	.126	1.376	.371	.356	1.606
p_o = 0.5	4.5	.189	1.774	.334	.319	2.140
	6.0	.252	2.162	.298	.283	2.140
$\bar{u}$ = .708	7.5	.315	2.540	.263	.248	2.680
fps	9.0	.378	2.920	.227	.212	3.210
$\frac{1}{2}\rho\bar{u}^2$ = .0934	10.5	.442	3.300	.192	.177	3.210
in. of	12.0	.504	3.675	.157	.142	3.750
H_2O	13.5	.567	4.050	.122	.107	4.290
N_{Re} = 782	15.0	.630	4.430	.086	.071	4.290
	(Exit) 18.0	.756	5.190	.015	0	-
Obs No. 1-2						
	1.5	.047	.774	.522	.524	.903
p_o = .65	3.0	.095	1.152	.459	.461	1.204
	4.5	.142	1.482	.411	.413	1.505
$\bar{u}$ = .9435	6.0	.189	1.774	.356	.358	1.806
	7.5	.236	2.061	.308	.310	2.108
$\frac{1}{2}\rho\bar{u}^2$ = .166	9.0	.284	2.350	.260	.262	2.410
	10.5	.331	2.636	.213	.215	2.710
N_{Re} = 1042	12.0	.378	2.920	.165	.167	3.010
	13.5	.425	3.200	.118	.120	3.010
	15.0	.473	3.485	.072	.074	3.310
	(Exit) 18.0	.567	3.930	-.002	0	-
Obs No. 1-3						
	1.5	.032	.639	.860	.855	.666
p_o = 1.10	3.0	.063	.918	.756	.751	.933
	4.5	.095	1.152	.668	.663	1.200
$\bar{u}$ = 1.416	6.0	.126	1.376	.584	.579	1.334
	7.5	.158	1.575	.510	.505	1.600
$\frac{1}{2}\rho\bar{u}^2$ = .375	9.0	.189	1.774	.435	.430	1.866
	10.5	.221	1.967	.363	.358	2.000
N_{Re} = 1564	12.0	.252	2.162	.289	.284	2.135
	13.5	.284	2.350	.219	.214	2.400
	15.0	.315	2.540	.148	.143	2.535
	(Exit) 18.0	.378	2.920	.005	0	-

Obs No. 2-1	x	X	Analytical $\frac{p_o-p}{\frac{1}{2}\rho\bar{u}^2}$	p	p corrected for exit error	Experimental $\frac{p_o-p}{\frac{1}{2}\rho\bar{u}^2}$
	1.5	.0243	.498	1.087	1.111	.478
p_o=1.4	3.0	.0486	.737	.938	.962	.718
$\bar{u}$=1.834	6.0	.0972	1.094	.714	.738	1.038
$\frac{1}{2}\rho\bar{u}^2$=.627	9.0	.1458	1.411	.515	.539	1.356
N_{Re}=2028	12.0	.1944	1.698	.335	.359	1.675
	15.0	.243	1.984	.156	.180	1.915
(Exit)	18.0	.2916	2.271	-.024	0	-
Obs No. 2-2	1.5	.0486	.692	.491	.473	.956
	3.0	.0972	1.034	.438	.420	1.275
p_o= .6	6.0	.1914	1.600	.349	.331	1.600
$\bar{u}$= .917	9.0	.2815	2.074	.275	.257	2.230
$\frac{1}{2}\rho\bar{u}^2$=.157	12.0	.388	2.660	.182	.164	2.870
N_{Re}=1014	15.0	.486	3.180	.100	.082	3.180
(Exit)	18.0	.583	3.710	.018	0	-
Obs No. 3-1	1.5	.0396	.634	.650	.591	.636
	3.0	.0792	.918	.584	.525	.848
p_o= .8	6.0	.1585	1.411	.467	.408	1.483
$\bar{u}$= 1.125	9.0	.238	1.850	.363	.304	1.906
$\frac{1}{2}\rho\bar{u}^2$=.236	12.0	.317	2.280	.262	.203	2.330
N_{Re}= 1243	15.0	.396	2.710	.160	.101	2.760
(Exit)	18.0	.476	3.140	.059	0	-
Obs No. 3-2	1.5	.0594	.733	.423	.359	.955
	3.0	.1188	1.091	.386	.322	.955
p_o = .5	6.0	.238	1.724	.319	.255	1.91
$\bar{u}$ = .75	9.0	.3565	2.340	.255	.191	2.385
$\frac{1}{2}\rho\bar{u}^2$ = .1048	12.0	.4755	2.945	.191	.127	2.862
N_{Re} = 828	15.0	.594	3.550	.128	.064	3.820
(Exit)	18.0	.713	4.160	.064	0	-
Obs No. 4-1	1.5	.0314	.550	.794	.769	.534
	3.0	.063	.800	.700	.675	.800
p_o = 1.0	6.0	.126	1.210	.546	.521	1.334
$\bar{u}$ = 1.416	9.0	.189	1.575	.410	.385	1.600
$\frac{1}{2}\rho\bar{u}^2$ = .375	12.0	.252	1.920	.280	.255	2.000
N_{Re} = 1564	15.0	.315	2.260	.152	.127	2.400
(Exit)	18.0	.378	2.600	.025	0	-
Obs No. 4-2	1.5	.0473	.626	.496	.462	.603
	3.0	.0945	.952	.442	.408	1.206
p_o = .6	6.0	.189	1.479	.355	.321	1.508
$\bar{u}$ = .9435	9.0	.2835	1.966	.274	.240	2.110
$\frac{1}{2}\rho\bar{u}^2$ = .166	12.0	.378	2.448	.193	.159	2.415
N_{Re} = 1042	15.0	.4725	2.930	.113	.079	3.015
(Exit)	18.0	.567	3.410	.034	0	-

	x	X	Analytical $\frac{p_o - p}{\frac{1}{2}\rho \bar{u}^2}$	p	p corrected for exit error	Experimental $\frac{p_o - p}{\frac{1}{2}\rho \bar{u}^2}$
Obs No. 5-1	1.5	.0431	.745		1.088	.567
p_o = 1.35	3.0	.0862	1.105		.961	.993
$\bar{u}$ = 1.376	4.5	.1294	1.415		.852	1.280
$\frac{1}{2}\rho \bar{u}^2$ =.352	6.0	.1725	1.700		.752	1.420
N_{Re} = 1114	7.5	.2160	1.964		.658	1.850
	9.0	.2590	2.235		.564	2.270
	10.5	.3020	2.504		.468	2.555
	12.0	.3450	2.770		.375	2.700
	13.5	.3880	3.030		.282	2.980
	15.0	.4310	3.300		.190	3.260
	(Exit) 18.0	.5180	3.830		0	3.830
Obs No. 5-2	1.5	.0331	.609		1.418	.558
	3.0	.0662	.877		1.25	.797
p_o = 1.8	6.0	.1325	1.335		.964	1.276
$\bar{u}$ = 1.834	9.0	.1986	1.735		.710	1.752
$\frac{1}{2}\rho \bar{u}^2$ = .627	12.0	.2650	2.120		.470	2.080
N_{Re} = 1486	15.0	.3310	2.496		.235	2.470
	(Exit) 18.0	.3970	2.875		0	-
Obs No. 5-3	1.5	.0540	.742	.825	.785	.635
	3.0	.1080	1.114	.737	.697	1.060
p_o = 1.0	6.0	.2160	1.730	.592	.552	1.695
$\bar{u}$ = 1.125	9.0	.3240	2.315	.454	.414	2.330
$\frac{1}{2}\rho \bar{u}^2$ = .236	12.0	.4320	2.905	.314	.274	2.960
N_{Re} = 911	15.0	.5400	3.485	.178	.138	3,390
	(Exit) 18.0	.6480	4.065	.04	0	-
Obs No. 5-4	1.5	.0644	.758	.624	.614	
	3.0	.1288	1.136	.561	.551	
p_o = .75	6.0	.2580	1.834	.446	.436	
$\bar{u}$ = .943	9.0	.3870	2.490	.336	.326	
$\frac{1}{2}\rho \bar{u}^2$ = .166	12.0	.5160	3.150	.227	.217	
N_{Re} = 763	15.0	.6440	3.800	.120	.110	
	(Exit) 18.0	.7730	4.460	.01	0	

App. V-4

Sample calculations for Observation No. 2-2

The pertinent data were as follows :

Observation No. 2-2 ; Working liquid : Water.

Flow-rate, Q = 3 lbs 14 ozs per 20 seconds of collection.

Wall speed, u_w = 0.1833 fps.

Channel gap, 2h = 0.122 inches.

Channel width = 4.01 inches.

Operating Temperature = 81°F.

From property tables for water,

Density, ρ = 62,2 lbs/ft^3

Kinematic viscosity, ν = 0.92×10^{-5} ft^2/sec.

Taps	2	3	4	6	8	10	12	Exit
Axial distance, x in inches.	0.0	1.5	3.0	6.0	9.0	12.0	15.0	18.0
Static pressure in inches of Water at 81°F.	0.6	.45	.40	.35	.25	.15	.10	

Calculations :

Flow-rate, Q = .003115 cfs.

Average velocity, $\bar{u}$ = .003115 x 144 / .122 x 4.01 = .917 fps.

Wall speed, u_W = .1833 fps.

$\omega_w = u_w / \bar{u} = .1833 / .917 \simeq .2$

$\frac{1}{2}\rho\bar{u}^2 \equiv \bar{u}^2 / 2g$ ft of Water = .157 inch of Water.

For tap No. 3,

Axial distance, x = 1.5"

Dimensionless axial co-ordinate, $X = \frac{x \nu}{\bar{u} h^2} = .0486$

$\frac{(P_o - P)_{fd}}{\frac{1}{2}\rho\bar{u}^2} = 3(2 - \omega_w)\ X = 5.4X = .262$

From graph, K(x) = .43

Therefore, $\frac{P_o - P}{\frac{1}{2}\rho\bar{u}^2} = .262 + .43 = .692$

Therefore, $p_o - p = .692 \times .157 = .109$ inch of Water

Therefore, p = .6 - .109 = .491 inch of Water

The rest of the calculations for other tap sections are tabulated in App. V-3.

The exit error for this set of readings came out to be + .018 inch of Water.

Therefore, analytical pressure at tap 3 with exit error correction,

p = .491 - .018 = .473 inch of Water.

Similarly other pressures at the other taps are corrected.

The Reynold's number, $N_{Re} = \bar{u} \cdot 2h / \nu = .917 \times .122 / 12 \times .92 \times 10^{-5}$

$= 1014.$

Pressure gradient from basic equations :

The slope of the pressure curve in the fully developed region, as derived in Ch.III from basic equations of motion is given by eqn. 39,

$dp/dx = 3(u_w - 2\bar{u}) = -.0274$ in. of Water per in. of axial distance.

dp/dx of the analytical pressure curve between last tap and the exit,

= -.082 / 3.0 = - .0273 in. of Water per in. of axial distance.

BIBLIOGRAPHY

1. Hagen G., Uber die Bewegung des Wassers in engen zylindrischen Rohren, Pogg. Ann 46, 423-442 (1839).

2. Poisseuille J., Recherches experimentelles sur le mouvement des liquids dans les tubes de tres petits diametres, Comptes Rendus 11, 961-967 and 1041-1048 (1840) : 12, 112-115 (1841).

3. Sparrow E.M. and Yu H.S., Flow Development in a Channel Having a Longitudinally Moving Wall, Trans ASME, J of App. Mech., June 1970.

4. Schiller L., Angew Z., Math. Mech. 2, 96 (1922)

5. Campbell W.D. and Slattery J.C., J of Basic Eng., 85, 41 (1963).

6. Boussinesq J., Compt. Rend., 113, 9, 49 (1891)

7. Schlicting H., Angew Z., Math. Mech. 14, 368 (1934).

8. Goldstein S., Modern Developments in Fluid Dynamics (Clarendon Press, Oxford, England , 1938) vol. 1, p 304.

9. Sparrow E.M., Lin H.S. and Lundgren T.S., Flow Development in the Hydrodynamic Entrance Region of Tubes and Ducts, The Physics of Fluids, vo. 7, No, 3, March 1964.

10. Sparrow E.M., Hixon C.W. and Shavit G., Experiments on Laminar Flow Development in Rectangular Ducts, Trans ASME, J of **Basic Eng.**, **March 1967**, pp 116-124.

11. Sparrow E.M., Flemming D.P., Flow in the Hydrodynamic Entrance Region of Ducts of Arbitrary Cross Section, Trans ASME, J of Heat Transfer, August 1969, pp 345-354.

12. Schlicting H, Boundary Layer Theory, Translated in English By J.Kestin, Sixth Edition, McGaw Hill Publications.